AEDC-TR-75-143

oy.?

STABILITY AND CONTROL TESTS OF A 0.05-SCALE RF-4C AIRCRAFT MODEL MODIFIED FOR FLIGHT TESTING THE AEDC 10-DEG TRANSITION CONE

PROPULSION WIND TUNNEL FACILITY
ARNOLD ENGINEERING DEVELOPMENT CENTER
AIR FORCE SYSTEMS COMMAND
ARNOLD AIR FORCE STATION, TENNESSEE 37389

January 1976

Final Report for Period April 2 — 5, 1975

Approved for public release; distribution unlimited.

Prepared for

DIRECTORATE OF TECHNOLOGY (DY)
ARNOLD ENGINEERING DEVELOPMENT CENTER
ARNOLD AIR FORCE STATION, TENNESSEE 37389

This report has been reviewed by the Information Office (OI) and is releasable to the National Technical Information Service (NTIS). At NTIS, it will be available to the general public, including foreign nations.

APPROVAL STATEMENT

This technical report has been reviewed and is approved for publication.

FOR THE COMMANDER

JOHN C. CARDOSI
Lt Colonel, USAF
Chief Air Force Test Director, PWT
Directorate of Test

CRAIG E. MAHAFFY
Colonel, USAF
Director of Test
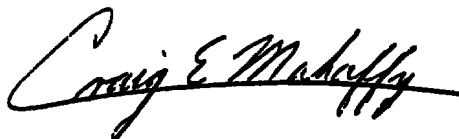
REPORT DOCUMENTATION PAGE		READ INSTRUCTIONS BEFORE COMPLETING FORM
1 REPORT NUMBER AEDC-TR-75-143	2 GOVT ACCESSION NO.	3 RECIPIENT'S CATALOG NUMBER
4. TITLE (and Subtitle) STABILITY AND CONTROL TESTS OF A 0.05-SCALE RF-4C AIRCRAFT MODEL MODIFIED FOR TESTING THE AEDC 10-DEG TRANSITION CONE		5 TYPE OF REPORT & PERIOD COVERED Final Report, April 2 - 5, 1975
		6 PERFORMING ORG REPORT NUMBER
7 AUTHOR(s) N. S. Dougherty, Jr. and A. C. Easterling, ARO, Inc.		8. CONTRACT OR GRANT NUMBER(s)
9 PERFORMING ORGANIZATION NAME AND ADDRESS Arnold Engineering Development Center (XO) Air Force Systems Command Arnold Air Force Station, TN 37389		10 PROGRAM ELEMENT, PROJECT, TASK AREA & WORK UNIT NUMBERS 65807F 921V 20
11 CONTROLLING OFFICE NAME AND ADDRESS Directorate of Technology (DYFS) Arnold Engineering Development Center Arnold Air Force Station, TN 37389		12. REPORT DATE January 1976
		13. NUMBER OF PAGES 50
14 MONITORING AGENCY NAME & ADDRESS(if different from Controlling Office)		15 SECURITY CLASS. (of this report) UNCLASSIFIED
		15a DECLASSIFICATION/DOWNGRADING SCHEDULE N/A

16 DISTRIBUTION STATEMENT (of this Report)

Approved for public release; distribution unlimited.

17. DISTRIBUTION STATEMENT (of the abstract entered in Block 20, if different from Report)

18 SUPPLEMENTARY NOTES

Available in DDC.

19 KEY WORDS (Continue on reverse side if necessary and identify by block number)

RF-4C aircraft
aerodynamics
static stability
transonic flow

20. ABSTRACT (Continue on reverse side if necessary and identify by block number)

An investigation of the aerodynamic characteristics of a 0.05-scale RF-4C aircraft was conducted in the AEDC 16-ft transonic Propulsion Wind Tunnel (16T) for the purpose of comparing a configuration with a Class II modification to that of the basic aircraft in preparation for flight testing. The Class II modification entailed the addition of a pivoting nose boom and the AEDC 3-ft-long, 10-deg transition cone to the nose of the aircraft. Data

DD FORM 1473 EDITION OF 1 NOV 65 IS OBSOLETE
1 JAN 73

20. ABSTRACT (Continued)

were taken at Mach numbers 0.20, 0.60, 0.80, 0.90, 0.97, 1.05, 1.20, and 1.50 at an angle-of-attack range from -4 to 24 deg and a sideslip angle range from -10 to 10 deg. Test results show very little change attributable to the addition of the cone for most of the aircraft speed range, this change falling within the range of measurement uncertainty for the test. Insufficient data were acquired to fully investigate the effects of the modification at low speeds, where the aircraft would be in its most critical attitudes; therefore, further tests of the aircraft at landing and approach speeds at high angles of attack are recommended.

AFSC
Arnold AFS Tenn

PREFACE

The work reported herein was conducted by the Arnold Engineering Development Center (AEDC), Air Force Systems Command (AFSC), at the request of the Aeronautical Systems Division (ASD/ENF) under Program Element 65807F. The results of the test were obtained by ARO, Inc. (a subsidiary of Sverdrup & Parcel and Associates, Inc.), contract operator of AEDC, AFSC, Arnold Air Force Station, Tennessee, under ARO Project Numbers P41S-29A and P32A-29A. The authors of this technical report were N. S. Dougherty, Jr. and A. C. Easterling. The manuscript (ARO Control No. ARO-PWT-TR-75-126) was submitted for publication on August 4, 1975.

CONTENTS

ILLUSTRATIONS

TABLES

1.0 INTRODUCTION

A static stability and control test was conducted in the transonic Propulsion Wind Tunnel (16T) at the Arnold Engineering Development Center (AEDC), in preparation for an aircraft modification to be performed by the Aeronautical Systems Division (ASD), 4950th Test Wing, Wright-Patterson Air Force Base, Ohio. The AEDC 10-deg transition cone (Refs. 1 through 3) is to be mounted on a pivotable nose boom of RF-4C aircraft Number 63-7744 and flight tested. A 0.05-scale model of the aircraft and cone was tested in 16T to ensure that the addition of the cone to the aircraft would not deteriorate the stability characteristics in such a way as to make the flight test unsafe. For more accurate comparisons of data, both a basic configuration and a modified version of the model aircraft were tested. Special attention was given to low-speed configurations at high angle of attack. It was impossible to simulate a realistic landing mode, however. because the aircraft model was not equipped with either flaps or landing gear. Effects of the cone on drag in the transonic region were also examined.

The test was in direct support of the proposed modification of the subject flight test aircraft nose structure to accept a pivoting nose boom and the 3-ft-long cone, which has a traversing pitot probe for detecting boundary-layer transition location on the cone surface in flight. The nose boom pitch angle is to be varied in order to compensate for changes in aircraft angle of attack with Mach number and altitude so that the cone can be positioned at zero angle of incidence. This installation will constitute a Class II modification to the aircraft.

2.0 APPARATUS

2.1 TEST FACILITY

Tunnel 16T is a closed-loop, continuous flow, variable density tunnel with a Mach number range from 0.20 to 1.60. The test section is 16 ft square and 40 ft long and is formed by fixed, parallel top and bottom perforated walls and variable angle perforated side walls.

This test utilized the standard 16T sting support system (Cart 2) in conjunction with the auxiliary pitch mechanism, which gave an angle-of-attack range from -6 to 24 deg. The roll angle range covered ±180 deg to allow upright and inverted operation as well as yaw angle variation of ±10 deg. A schematic of the test section with model installed is shown in Fig. 1, and photographs of the installed model are shown in Fig. 2.

2.2 TEST ARTICLES

A 0.05-scale model of the AEDC 10-deg transition cone complete with traversing pitot probe mechanism and flow-angle-sensing probe (Fig. 3) was fabricated from stainless steel for the test. Also fabricated was an aluminum RF-4C nose with detachable tips. One tip was the standard RF-4C radome configuration and was used to acquire baseline data. The proposed Class II modified nose configuration had a slot into which the adapters fit to set the pivotable nose boom at -2 and -6 deg relative to the model water reference line. A 0.05-scale complete model of the F-4 aircraft was available which had previously been tested in other configurations in the AEDC Aerodynamic Wind Tunnel (4T). Horizontal stabilator angle on the model was set manually using a leveling plate and an inclinometer. All horizontal stabilator angles were referenced to the model water reference line. The aircraft/cone model assembly with internal balance was as shown in Fig. 4. Figure 5 shows the locations of transition strips on the model. Number 120 grit size at 150 grains per linear inch was applied to both sides of the model wings, horizontal stabilators, and vertical stabilator. Grit was also applied on the intake ducts and on the nose.

2.3 INSTRUMENTATION

Aerodynamic loads on the model were measured with the Propulsion Wind Tunnel Facility (PWT) 4T 1.75 balance, which is a moment-type, six-component, internal strain-gage balance. Outputs from the balance were recorded on an oscillograph to monitor the model dynamics and on magnetic tape for data reduction. On-line data were also obtained using a cathode ray tube (CRT) graphics display in conjunction with the Raytheon 520 facility computer. The central IBM 370/75 computer was utilized for off-line recalculate capability and final computation of forces and moments.

Model base and balance cavity pressures were measured using 5-psia pressure transducers. The cavity pressure sensing point was located adjacent to the sting at the base of the balance. Because the model had no clearly defined base it was necessary to place the base pressure transducer inside the model cavity halfway between the engine exhaust nozzle and the balance. These locations were the same as those used in previous tests. The measurements of base pressure thus obtained were converted to force and used in computing forebody coefficients.

3.0 TEST PROCEDURES

3.1 TEST DESCRIPTION

Data were obtained on the RF-4C base configuration and the modified configuration with a cone angle of -2 deg at Mach numbers 0.20, 0.60, 0.90, 0.97, 1.05, 1.20, and

1.50. A cone angle of -6 deg was also tested at M_∞ = 0.20. During the flight test the cone will be kept at the smallest incidence angle to the flow possible; only at low air speeds is the trim angle of attack high enough to warrant dropping the cone through such a large angle. Additional excursions from -4 to 24 deg angle of attack were made at all Mach numbers for horizontal stabilator deflection angles (δ_s) of -5, -2, 0, 2, and 5 deg. A stabilator setting of δ_s = -20 deg at M_∞ = 0.20 was also tested. Sideslip angle excursions from 10 to -10 deg were taken at 0- and 5-deg angles of attack for horizontal stabilator deflections of 0 and -20 deg.

Prior to the initiation of tunnel operation during each test period, the model and balance were heated to the approximate temperature the balance would reach during the tunnel operation. This was done to reduce any temperature effects on the balance and to minimize balance instrumentation zero shifts.

3.2 DATA REDUCTION

Measured forces and moments were corrected for weight tare effects and used to calculate aerodynamic coefficients in the body and stability axis systems based on a reference area (S) of 1.325 sq ft and a reference mean aerodynamic chord length ($\bar{c}$) of 0.802 ft. Pitching, yawing, and rolling moments were transferred to the location of the center of gravity on the full-scale aircraft, which is at $0.31\bar{c}$. Measured axial-force and drag data were corrected for base and cavity pressures to obtain the forebody coefficients of these aerodynamic parameters. These coefficients were based on a cavity area of 0.0172 sq ft and a base area of 0.07465 sq ft.

Measurements for flow angularity in the vertical plane were taken on the basic model configuration at each test Mach number at roll angles of 0 and 180 deg. All model angle-of-attack data were corrected for relative flow angularity based upon these measurements. Corrections were also made for flow angle in the horizontal plane of the tunnel, using roll angles of 90 and -90 deg.

3.3 PRECISION OF MEASUREMENTS

Uncertainties (bands which included 95 percent of the calibration data) of the basic tunnel parameters (free-stream total pressure, p_t, total temperature, T_t, and free-stream Mach number, M_∞) were estimated from calibrations of the instrumentation and from the repeatability and uniformity of the test section flow during tunnel calibration. These estimates were then used to determine uncertainties of other free-stream properties (free-stream static pressure, p_∞, and free-stream dynamic pressure, q_∞) using the Taylor series method of error propagation. The estimated uncertainties are given in Table 1.

Calibrations of model angle of attack, sideslip angle, and roll angle are considered precise within ±0.1 deg.

The balance uncertainties, determined during the balance calibration, were combined with estimates of the tunnel parameter uncertainties, assuming a Taylor series propagation, to estimate the uncertainties of the aerodynamic coefficients. Uncertainties in C_L and C_D are presented at angles of attack of 0, 12, and 24 deg for free-stream Mach number $(M_\infty) = 0.20$ and at 0 and 12 deg for all other Mach numbers, since these are considered representative for the test conditions for which the majority of the data were obtained. Balance uncertainties are given in Table 2.

4.0 RESULTS AND DISCUSSION

4.1 GENERAL

Results are presented showing the effects of configuration changes on lift, pitching-moment, and drag coefficients. Sideslip data are also included showing the effects of configuration changes on directional stability. Data points shown in each figure represent values computed for trim conditions from the measurements made at varied δ_s values.

Trim conditions over a range of angles of attack were obtained at each Mach number for each configuration by cross plotting the lift coefficient (C_L) versus angle-of-attack curve, the lift coefficient versus pitching-moment coefficient curve (C_m), and the lift coefficient versus drag coefficient curve (C_D). Trim conditions required for level flight at each free-stream Mach number (M_∞) were determined mathematically on the basis of an aircraft weight supplied by the 4950th Test Wing of 33,000 lb at $M_\infty = 0.20$ and 36,000 lb at all other free-stream Mach numbers. However, these calculations incorporated the dynamic pressure (q_∞) that existed during the test rather than that for any particular flight altitude. Table 3 lists the test conditions.

Trim angles of attack for each free-stream Mach number were taken where the trim lift coefficient for level flight fell on the trim curves for coefficient of lift versus angle of attack. Trim deflection angle of the horizontal stabilator (δ_s) at each free-stream Mach number was determined by plotting horizontal stabilator deflection angle versus pitching-moment coefficient for that Mach number. Minimum drag coefficient $(C_{D_{min}})$, and the slopes of the lift curve (C_{L_α}), pitching-moment curve (C_{m_α}), rolling-moment curve (C_{ℓ_β}), side-force curve (C_{y_β}), and yawing-moment curve (C_{n_β}) were hand reduced from computer plots of these parameters.

4.2 LIFT AND DRAG CHARACTERISTICS

Comparisons of the lift and drag characteristics of the RF-4C model with and without the transition cone are presented in Figs. 6 through 9. Lift coefficient at zero pitching

moment as a function of angle of attack is shown for each Mach number in Fig. 6. Lift-drag curves at zero pitching moment are given in Fig. 7. Little or no difference can be seen in any of these data. However, the largest differences are noted to have occurred at Mach number 0.2 in the lift-drag curves, Fig. 7a. Slight differences in level and slope are evident in this case between the basic-cone off, modified-cone pitch angle of -2 deg, and modified-cone pitch angle of -6 deg configurations. At low angles of attack with low coefficients of lift and drag, the modified configurations appeared to have slightly less drag than the basic configurations, but at the higher angles of attack and the corresponding higher lift and drag coefficients the modified configurations seemed to have slightly more.

Slopes of the lift coefficient with angle of attack (C_{L_α}) are given as a function of Mach number in Fig. 8. As shown in Fig. 8, addition of the transition cone appears to reduce C_{L_α} nominally 1.5 percent throughout the test range of Mach numbers. Minimum drag coefficient ($C_{D_{min}}$), presented as a function of Mach number in Fig. 9, indicates a slight drag increase due to the presence of the cone of increment as large as 4 percent at subsonic conditions and 2-1/2 percent supersonic, which are only slightly higher than the measurement uncertainty values at the respective test conditions.

At Mach number 0.2 the model trimmed at a very high angle of attack, about 18 deg, which was dangerously close to the stall point of about 19 deg. This represented an unreasonable flight condition that would normally be compensated for by extension of flaps. Trim angle of attack (α_{trim}) is shown in Fig. 10 and was as low as 0.7 deg at Mach number 0.97. Trim angle of attack for the "cone on" case was nominally within 0.1 deg of that for the basic "cone off" case. It is seen from Fig. 10 that the arbitrary choice of -2 deg cone pitch position relative to the aircraft placed the cone at zero angle of incidence to the airflow near Mach number 0.6. The -6 deg stow position for the cone gives zero flow incidence at about Mach number 0.4. Through the transonic range, slightly greater pitch-up angles between 0 and -1 deg will probably be required in the full-scale flight test case to maintain zero cone incidence.

4.3 LONGITUDINAL STABILITY CHARACTERISTICS

Stabilator trim angle ($\delta_{s_{trim}}$) required for straight and level flight for these Mach numbers from 0.2 to 1.5 is shown in Fig. 11. No noticeable change in stabilator angle is indicated to achieve trim conditions with the transition cone installed.

The slope of the pitching-moment coefficient with angle of attack (C_{m_α}) at trim conditions is shown in Fig. 12 as a function of Mach number. The static margin is shown in Fig. 13. These data indicate no appreciable change in the longitudinal stability characteristics of the model with the cone installed. Static margin appears to attain a minimum value of about 6-1/2 percent of the mean aerodynamic chord at low subsonic

Mach numbers. Slight reduction in static margin by about 1-1/2 percent from that of the basic aircraft configuration is indicated in Fig. 13 at supersonic speeds.

4.4 DIRECTIONAL STABILITY CHARACTERISTICS

The directional stability characteristics for basic (cone off) and modified aircraft configurations are shown at angles of attack (a) of 0 and 5 deg, respectively. in Figs. 14 through 16. The slope of the yawing-moment coefficient with sideslip angle (C_{n_β}) is shown in Fig. 14 and differed slightly as shown for the absolute value of sideslip (β) greater than or less than 2 deg. Virtually no difference at all can be seen with the cone installed, in Fig. 14. Slight difference in side-force coefficient slope with sideslip angle (C_{Y_β}) is indicated at Mach number 0.2 in Fig. 15, where the side-force coefficient is approximately 1 percent lower.

A slight rolling moment existed at zero sideslip angle (β) in these data; this is attributable to a slight lateral flow angularity which is known to exist in the wind tunnel. Otherwise, the rolling-moment coefficient was symmetric about zero sideslip angle, and the slope of the rolling-moment coefficient with sideslip (C_{ℓ_β}) was as shown in Fig. 16. There appears to be a relatively large change in rolling-moment coefficient slope (C_{ℓ_β}) with angle of attack (a) but no appreciable change between basic and modified configurations.

5.0 CONCLUDING REMARKS

The results obtained in comparing the basic RF-4C model aircraft static stability and control characteristics with those obtained with the proposed Class II-modified configuration for the AEDC 10-deg transition cone to be mounted on a pivoting nose boom were that no appreciable difference could be found. All differences in lift and drag, pitching-. yawing-, and rolling-moment coefficients and side-force coefficient were either within or hardly more than the balance measurement uncertainty.
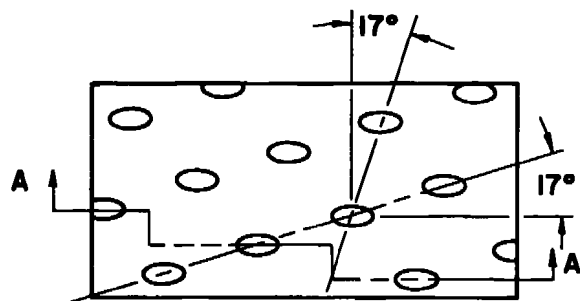
The lift coefficient slope with angle of attack appeared to be nominally 1.5 percent reduced. The minimum drag coefficient appeared to be increased by no more than 4 percent at subsonic conditions and 2-1/2 percent at supersonic conditions, which values are less than or only slightly higher than the balance measurement uncertainty at these conditions. There appeared to be a slight reduction in static margin by 1-1/2 percent at supersonic Mach numbers. No appreciable change in trim angle of attack or stabilator trim angle occurred. No change was noted in directional stability characteristics except that the side-force coefficient slope of the basic configuration was about 1 percent lower at Mach number 0.2 than was that of the modified configuration.

For the transonic and supersonic speed range up to Mach number 1.5 the subject tests have served to show that there is no appreciable change in the static stability and control characteristics for the aircraft. Neither is there very much change due to the addition of the cone for the low speeds.
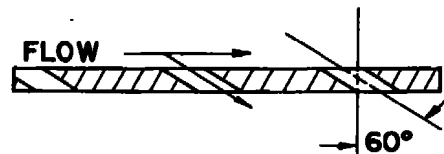
Insufficient data were obtained to examine fully any potential effects during an approach or landing, since the model was not equipped with flaps and landing gear. Data taken without flaps or gear in these tests yielded an unreasonably high trim angle of attack, dangerously close to the stall angle of attack of the aircraft (trim angle of 18 deg when the aircraft stalls at 19 deg), and an extremely high coefficient of drag at trim conditions for $M_\infty = 0.20$. Further tests to examine the effects of the cone at low speeds and high angles of attack with flaps and landing gear are therefore recommended.

REFERENCES

1. Credle, O. P. and Carleton, W. E. "Determination of Transition Reynolds Number in the Transonic Mach Number Range." AEDC-TR-70-218 (AD875995), October 1970.

2. Dougherty, N. S., Jr. and Steinle, F. W., Jr. "Transition Reynolds Number Comparisons in Several Major Transonic Tunnels." AIAA Paper No. 74-627, presented at the AIAA 8th Aerodynamic Testing Conference, Bethesda, Maryland, July 8-10, 1974.

3. Dougherty, N. S., Jr. "Prepared Comment on the Cone Transition Reynolds Number Data Correlation Study." Presented at the AGARD Fluid Mechanics Panel Symposium on Flight/Ground Testing Facilities Correlation, Valloire, France, June 9-13, 1975.

17°

FLOW

17°

60°

Section A-A

6% Open Area
Hole Diameter = 0.75 In.
Plate Thickness = 0.75 In.

TYPICAL PERFORATED
WALL PATTERN

SOLID DIVERGED WALL SECTION
TO ALLEVIATE STRUT BLOCKAGE

SOLID
AREA

PERFORATED
WALLS

MODEL SUPPORT
STRUT

STA
-10

STA
0

STA.
13.7

STA.
28

STA.
40

13

AEDC-TR-75-143
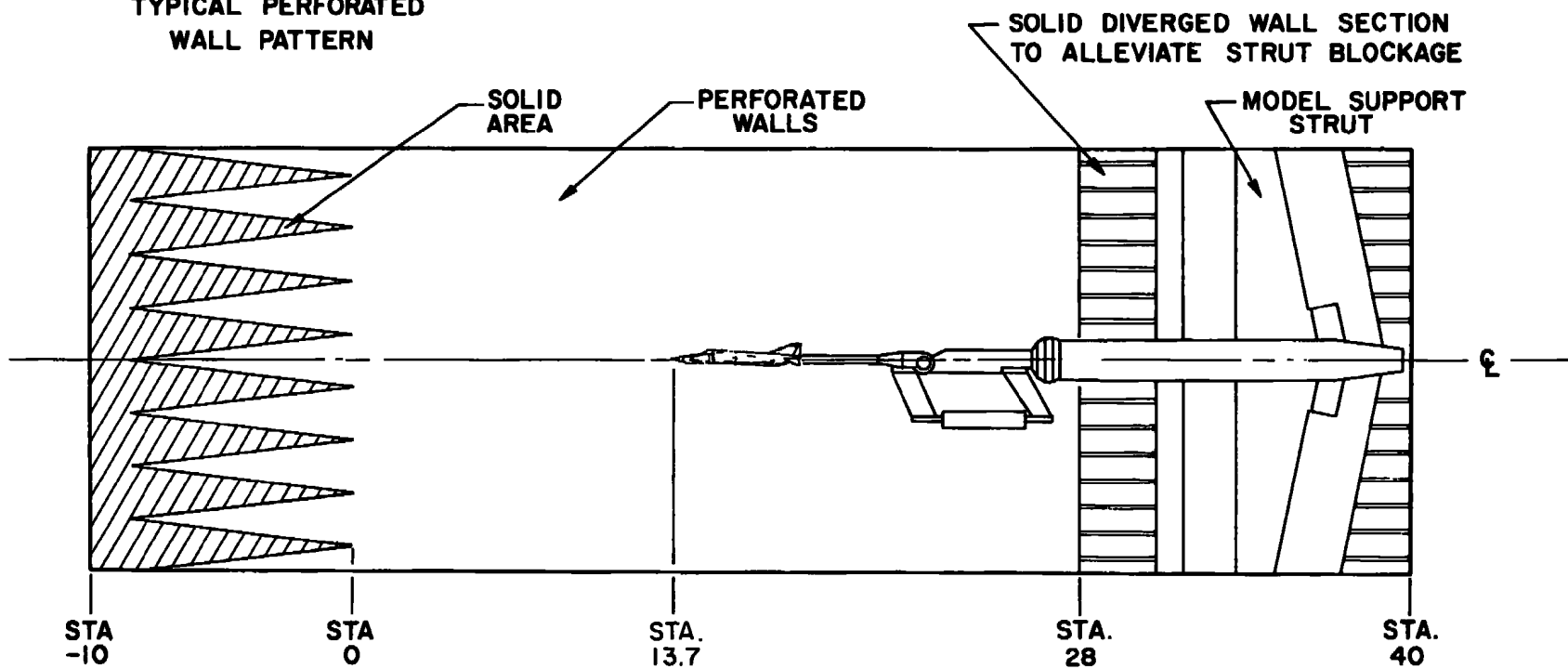
Figure 1. Sketch of model installation.
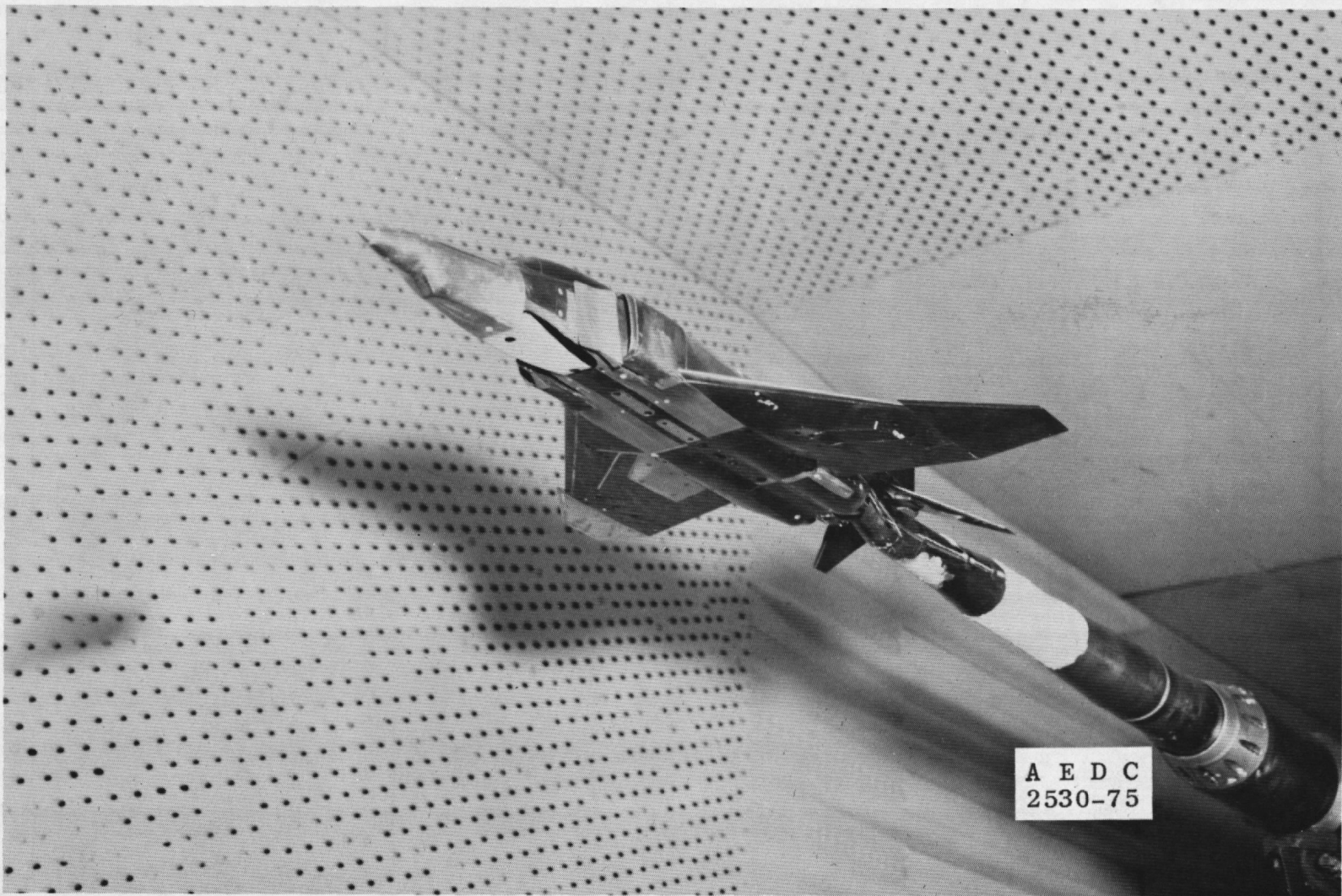
Figure 2. Photographs of model configurations.
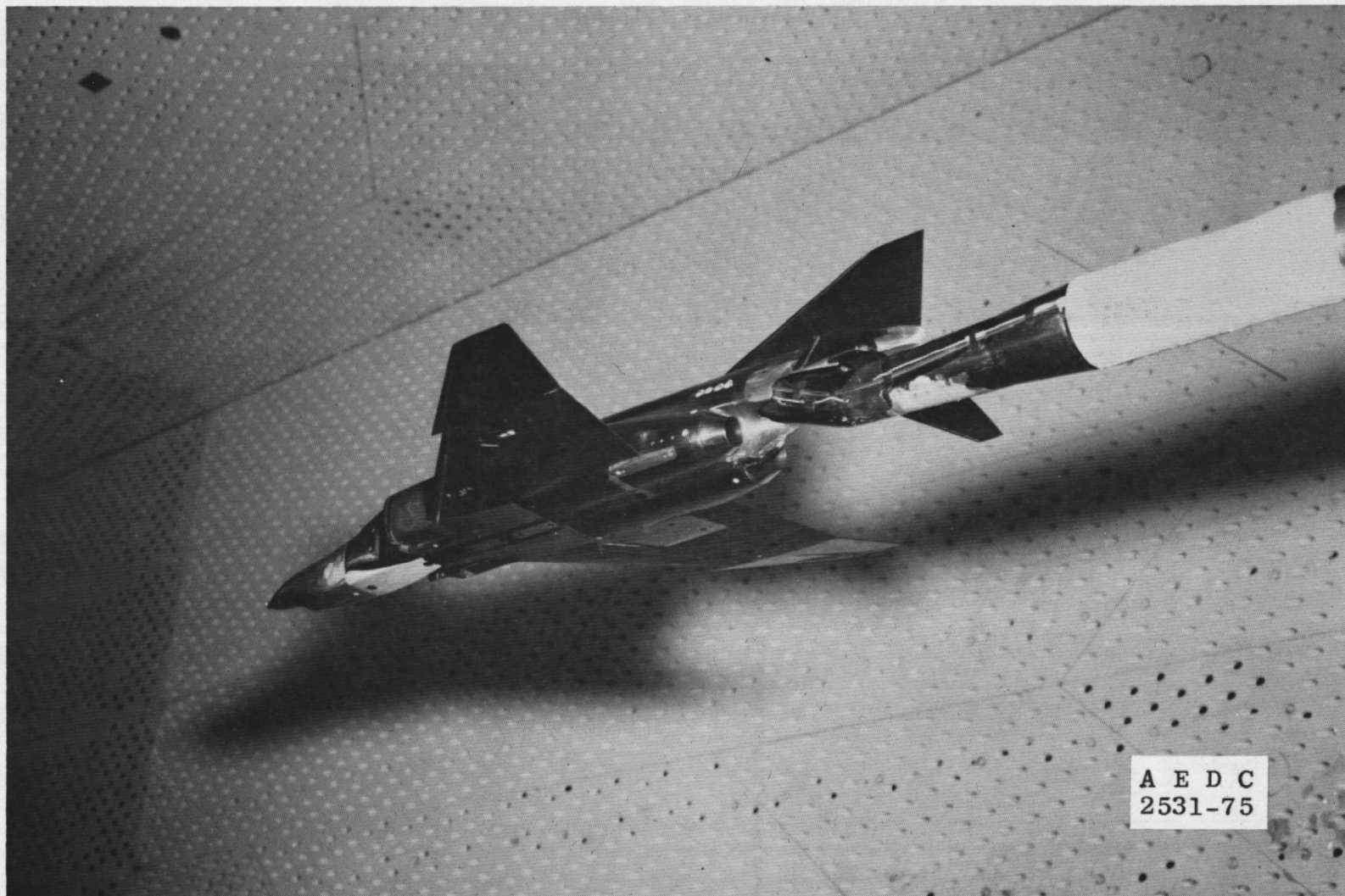
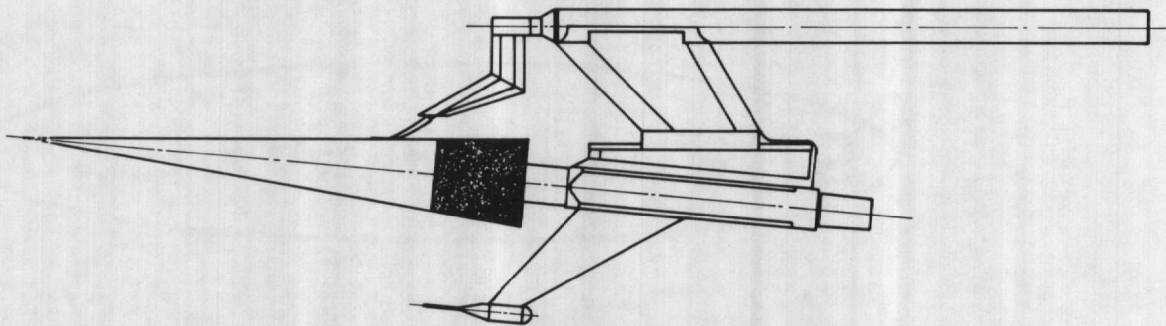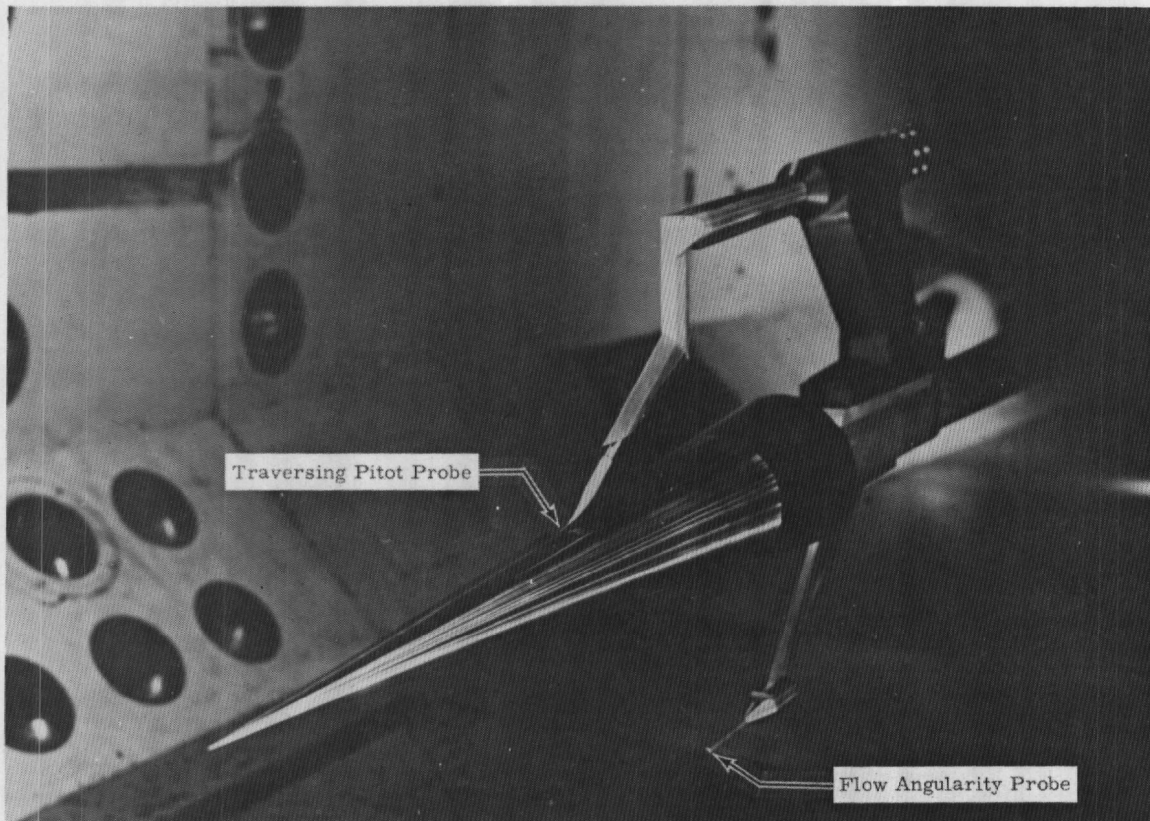Figure 2. Continued.
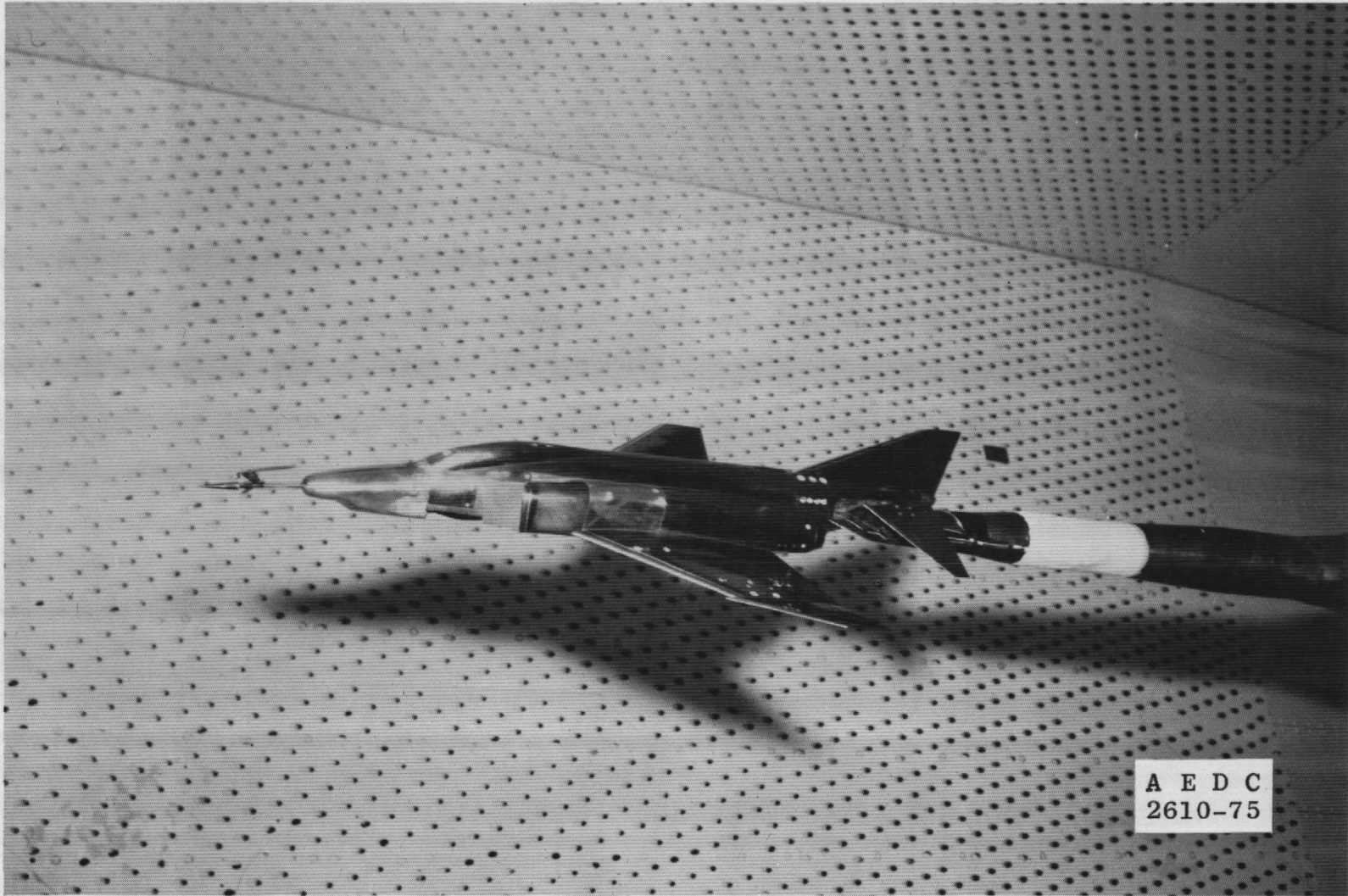
Figure 2. Continued.

Figure 2. Concluded.

Figure 3. Full-scale transition cone (to be flight tested).
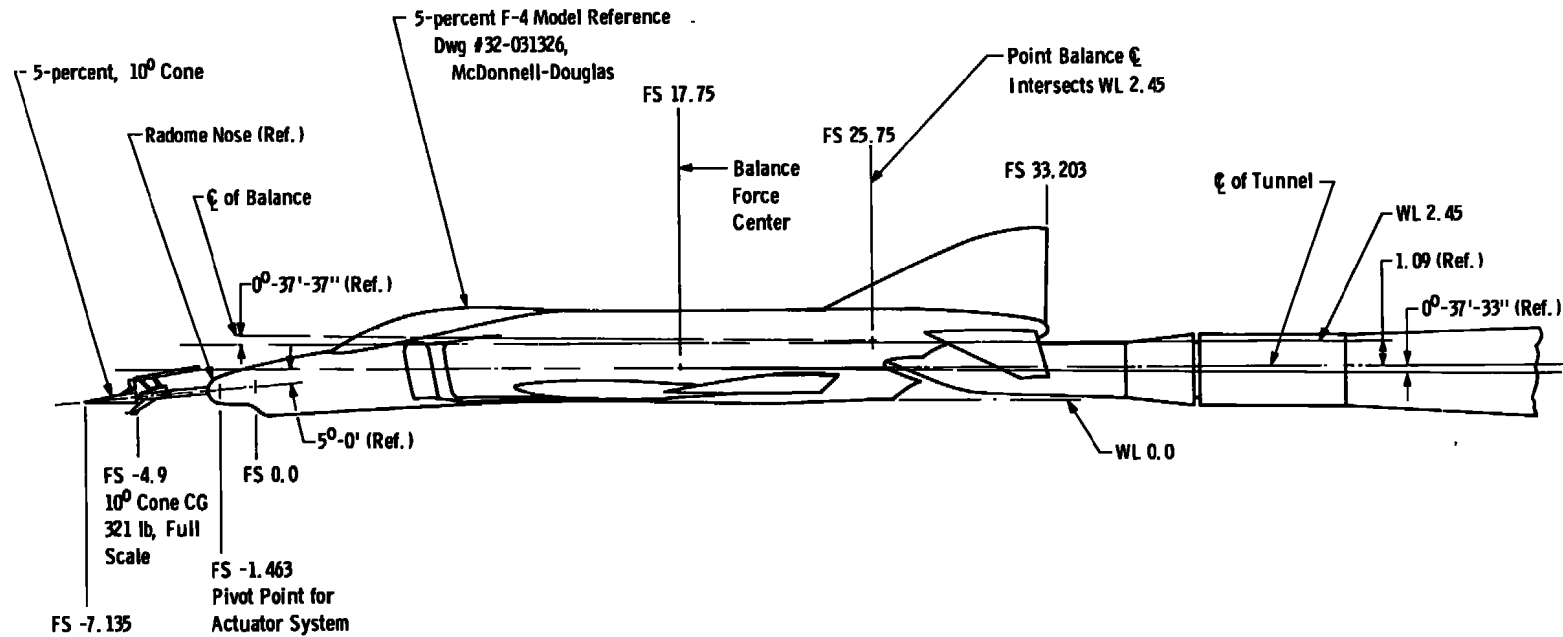
Figure 4. Model and balance dimensions.

0.10 (Typ)

0.75 (Typ)

0.25 (Typ)

0.10 (Typ)

Top View

Leading edge at 5-percent local
chord line. Typical of upper
and lower surfaces of unslatted
wings and horizontal tails, and
both sides of vertical tail.

Side View
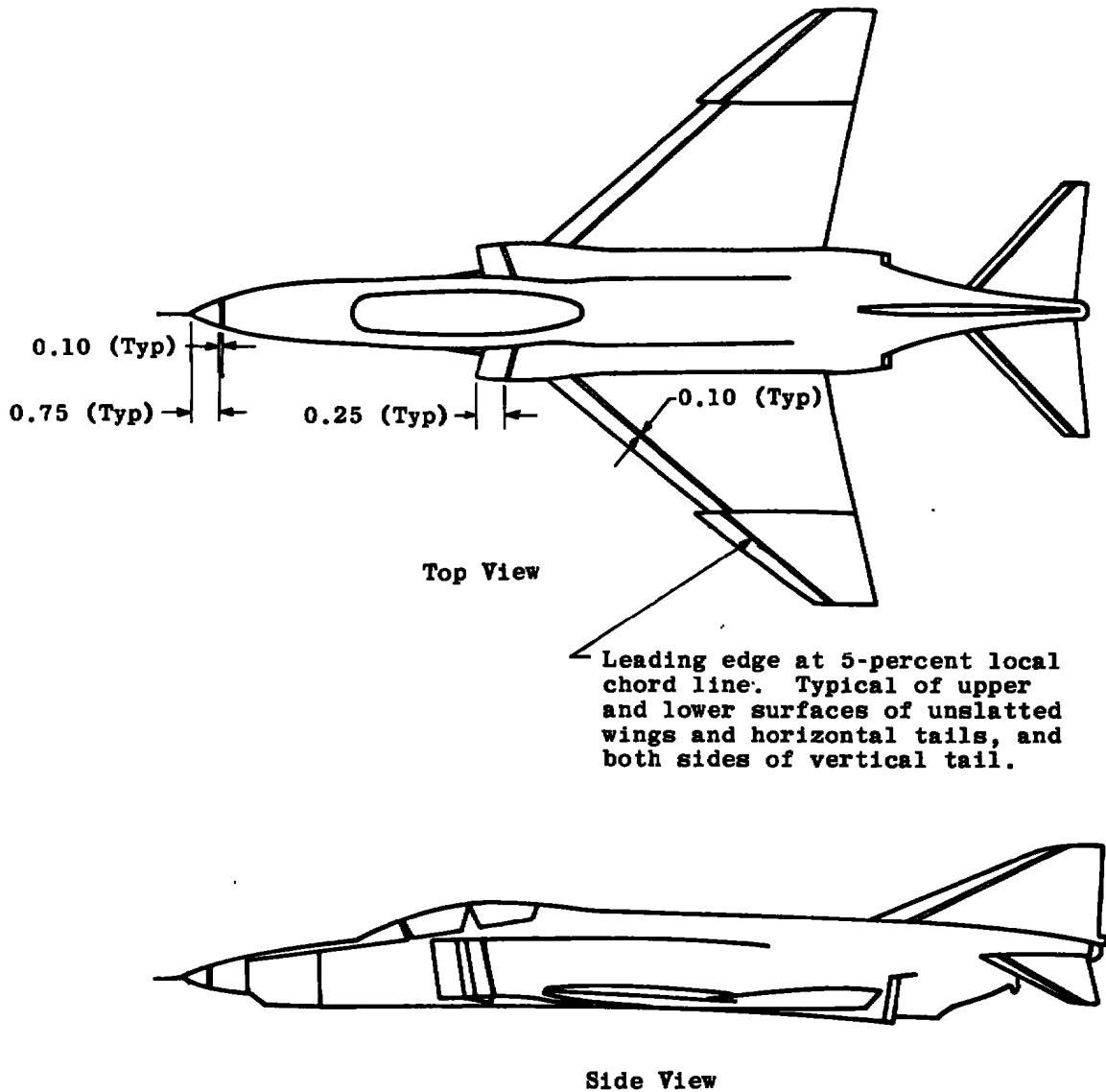
Notes: Grit size is No. 120.
          Density = 150 grains per linear inch.

Figure 5. Transition strip locations on the model.
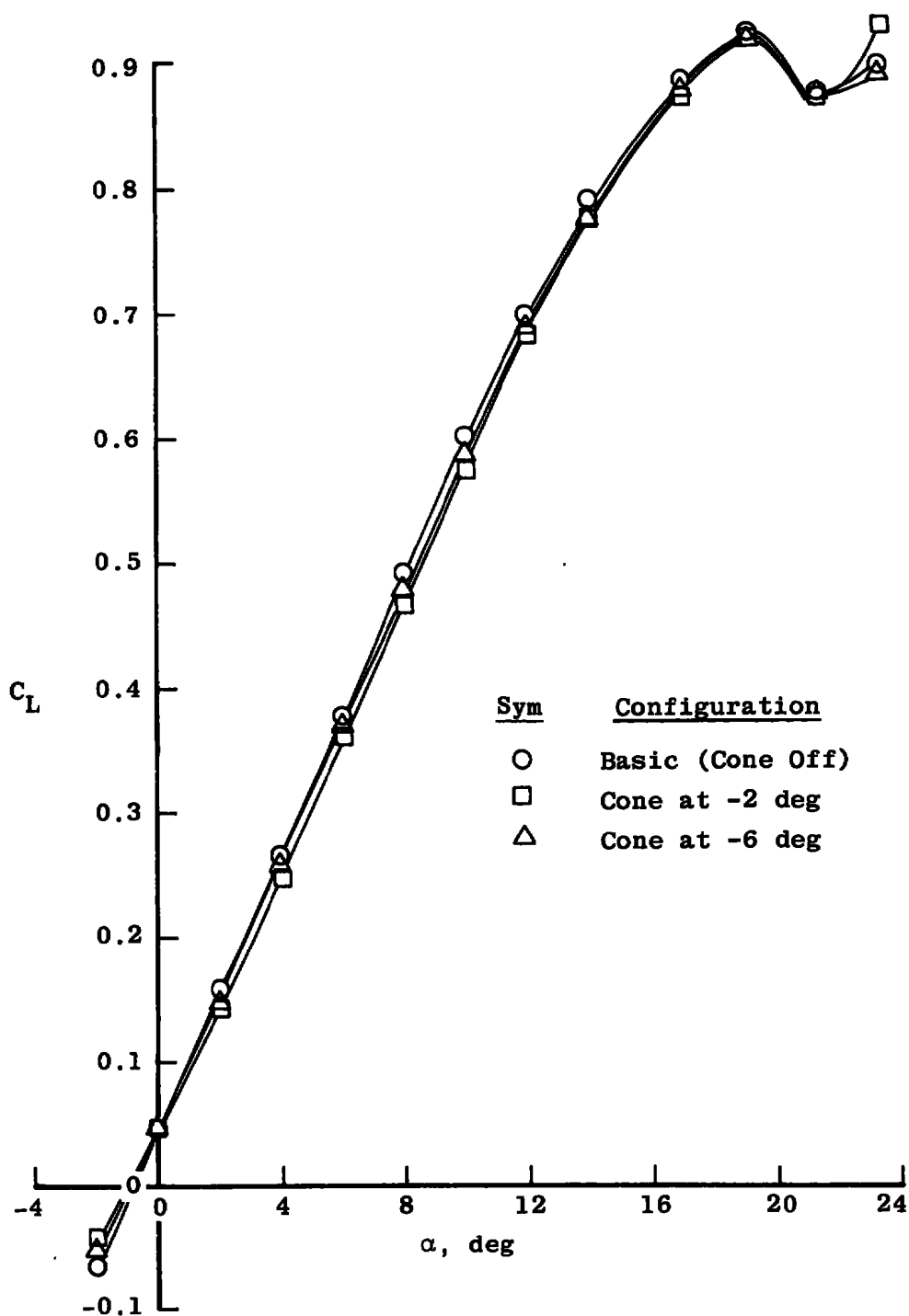
a. $M_\infty = 0.20$

Figure 6. Lift coefficient at zero pitching moment as a function of angle of attack.
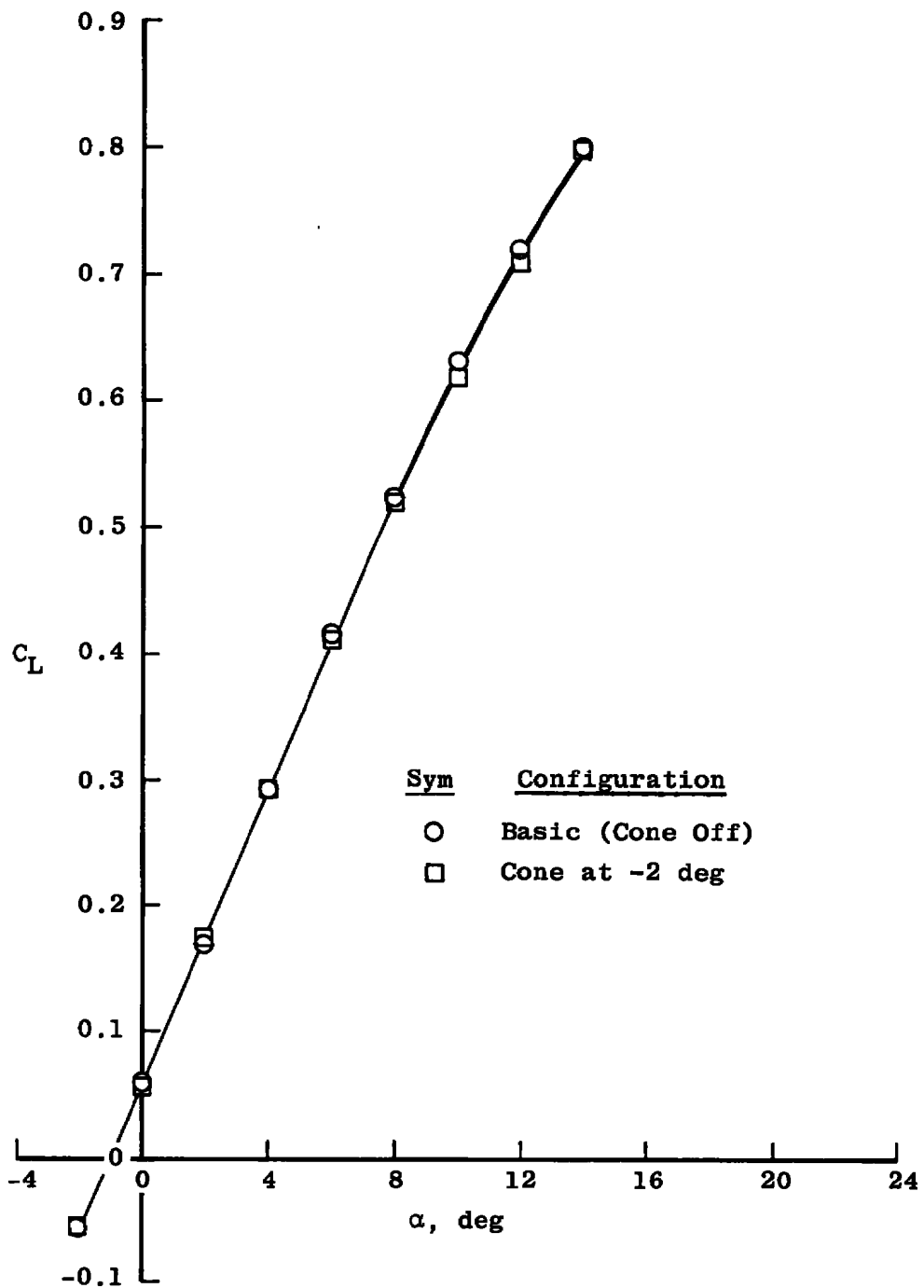
b. $M_\infty = 0.60$
Figure 6. Continued.
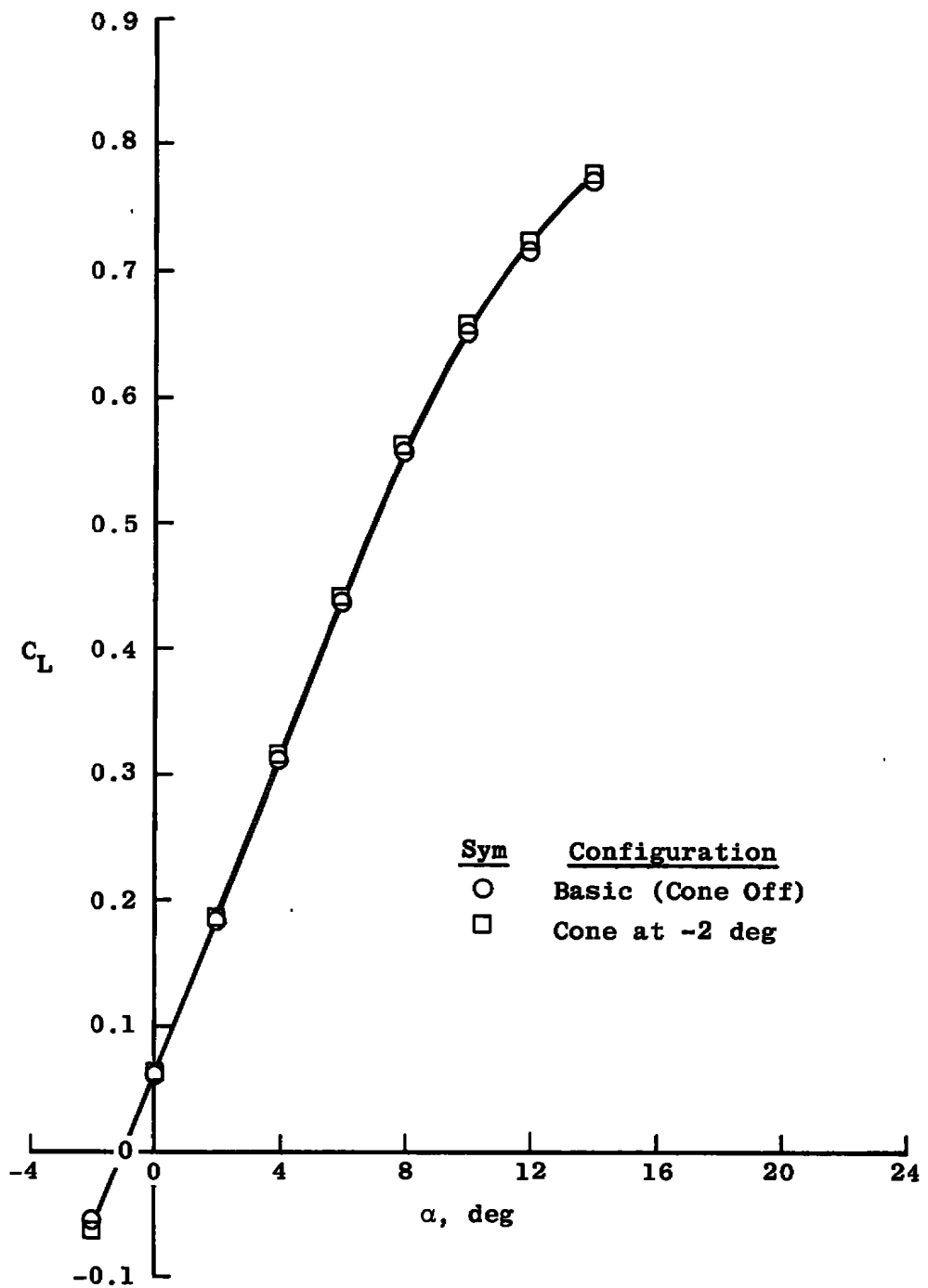
c. $M_\infty = 0.80$
Figure 6. Continued.
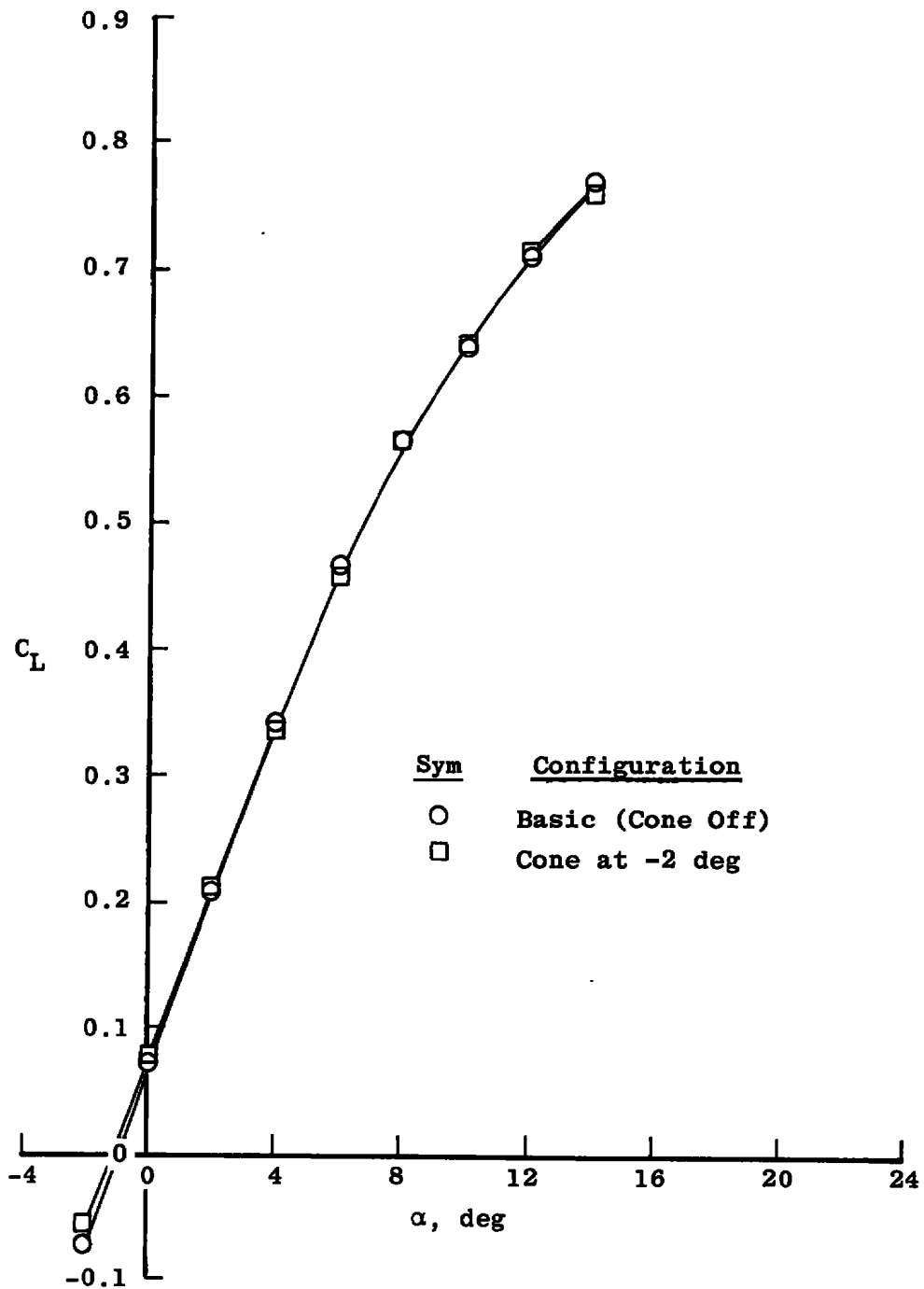
d. $M_\infty = 0.90$
Figure 6. Continued.
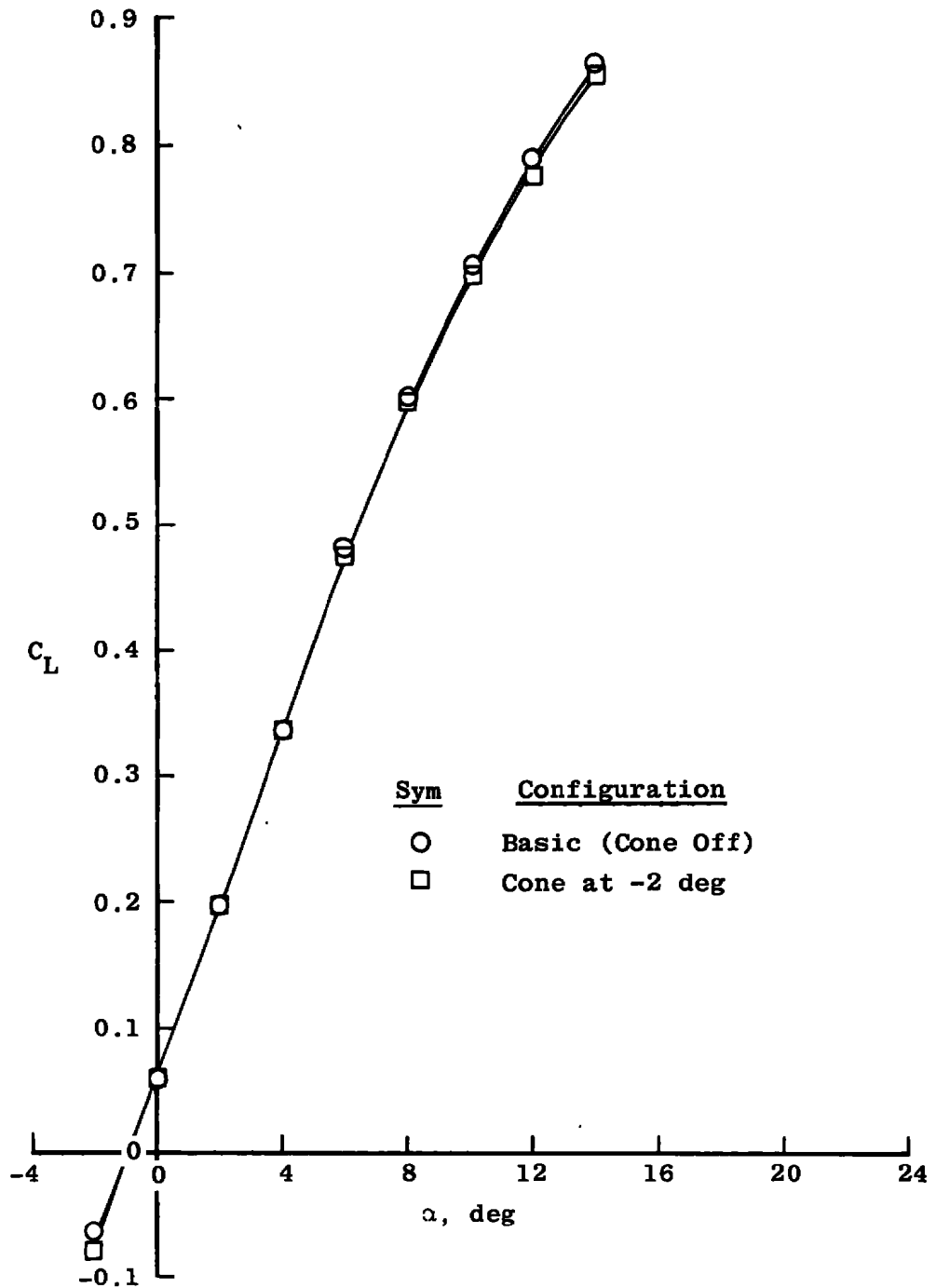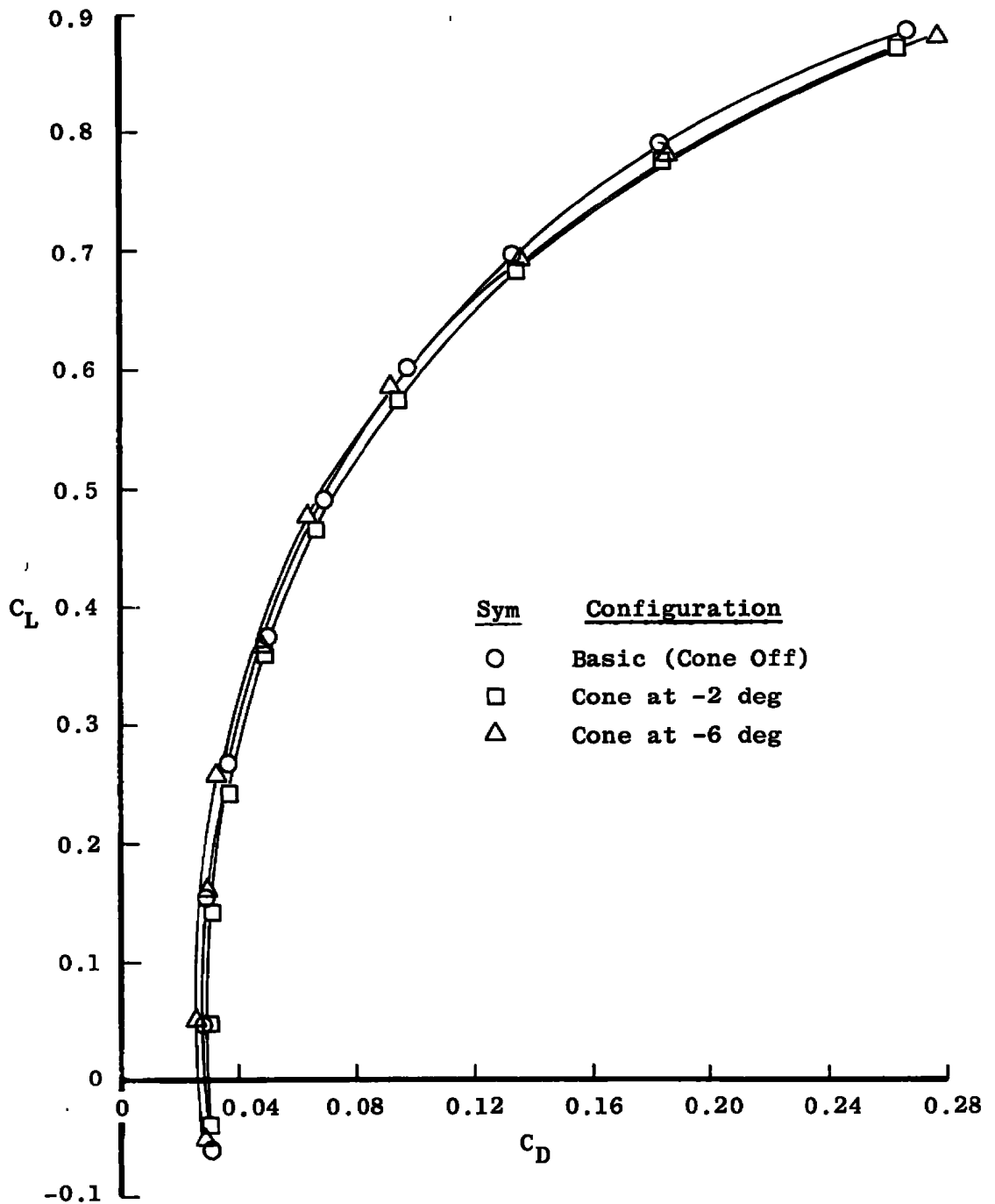
e. $M_\infty = 0.97$
Figure 6. Continued.
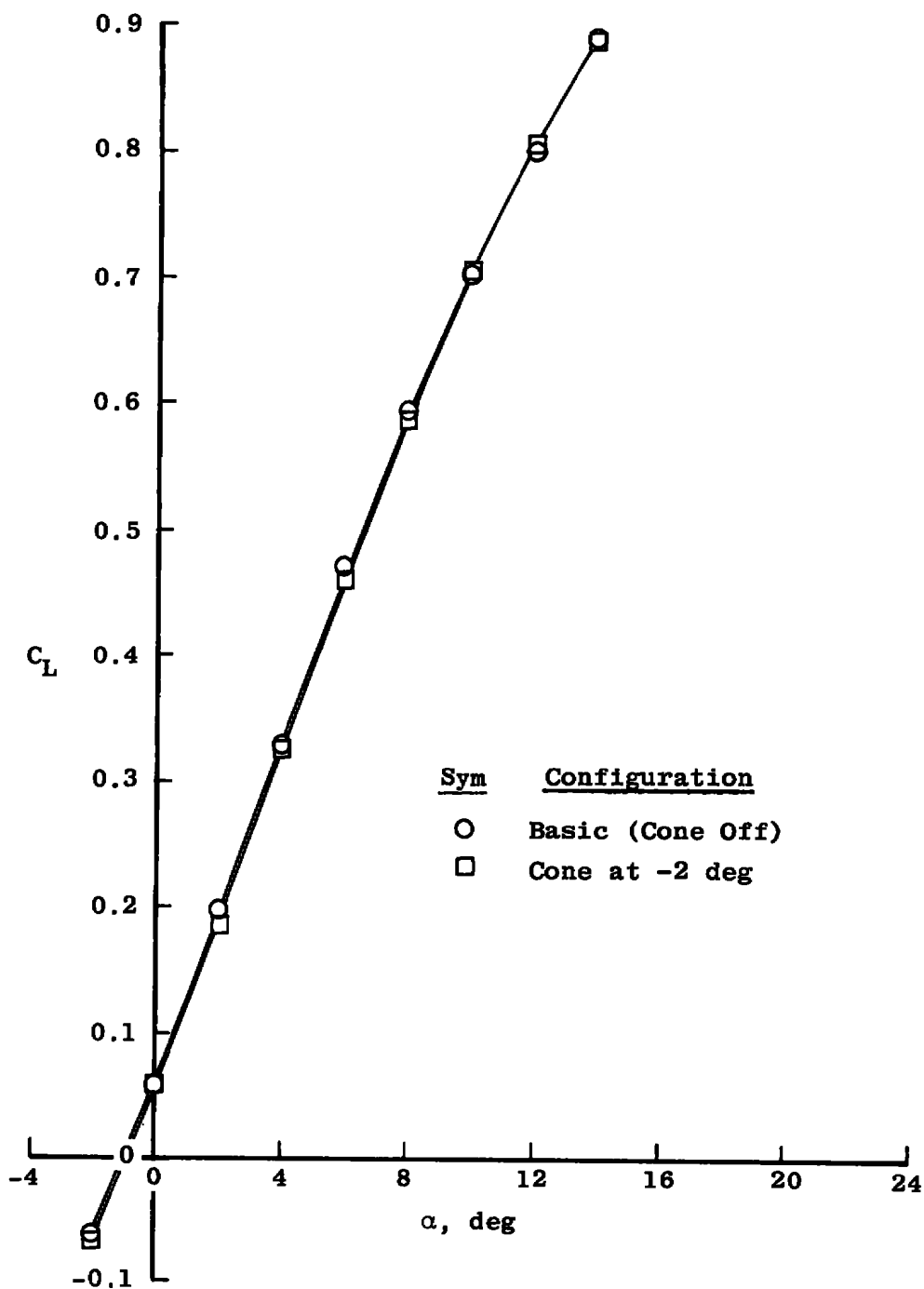
f. $M_\infty = 1.05$

Figure 6. Continued.
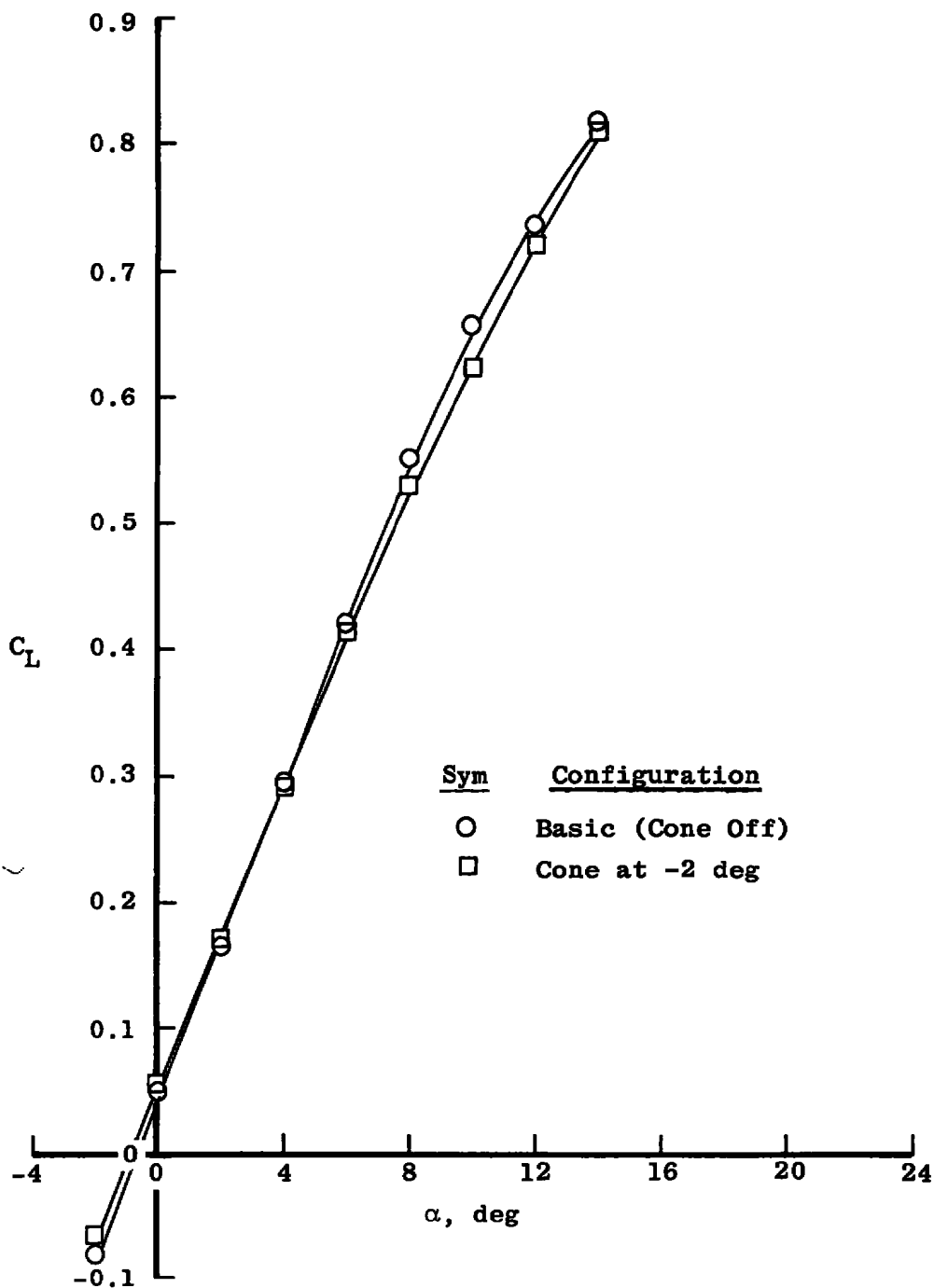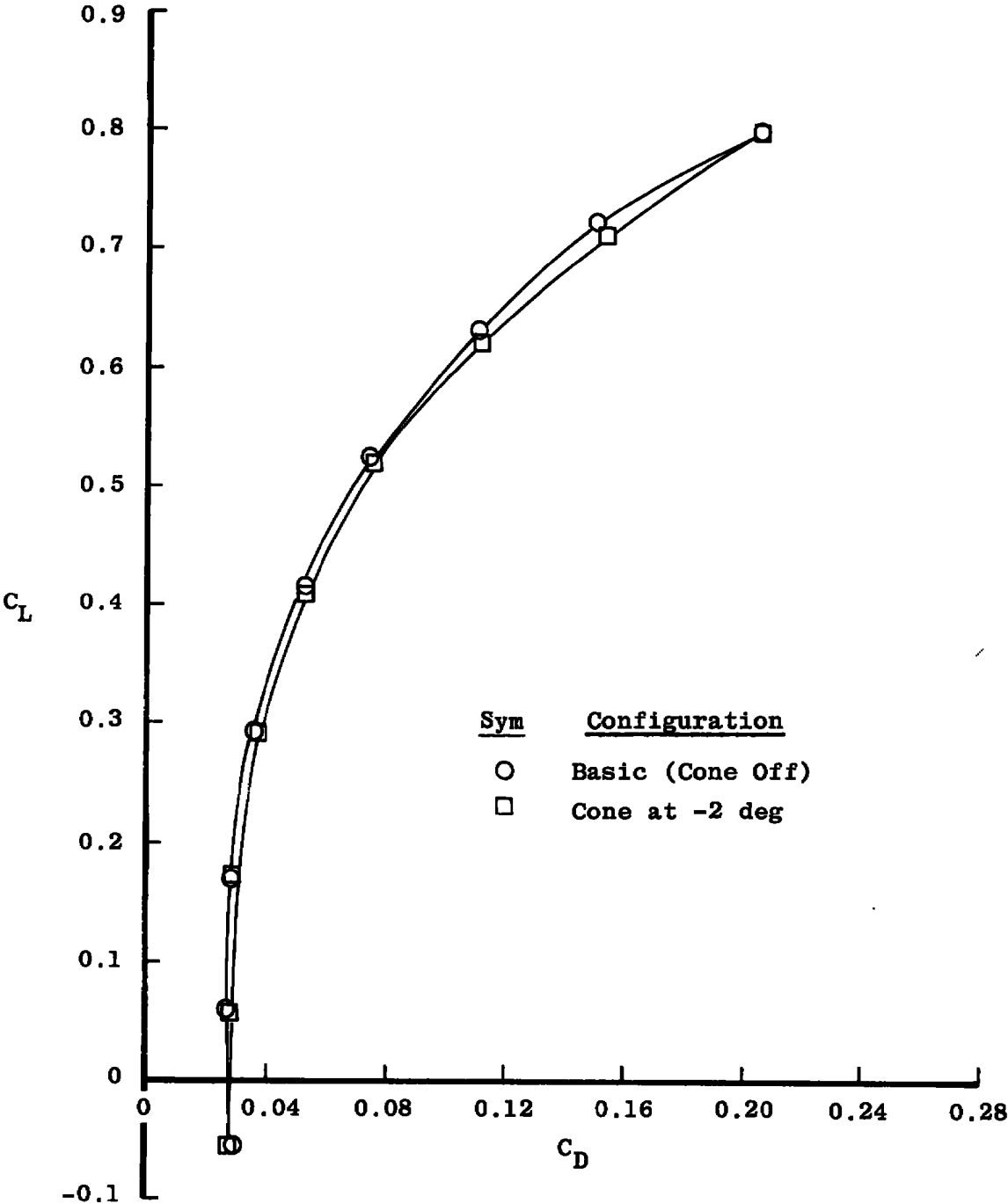
g. M_∞ = 1.20
Figure 6. Continued.
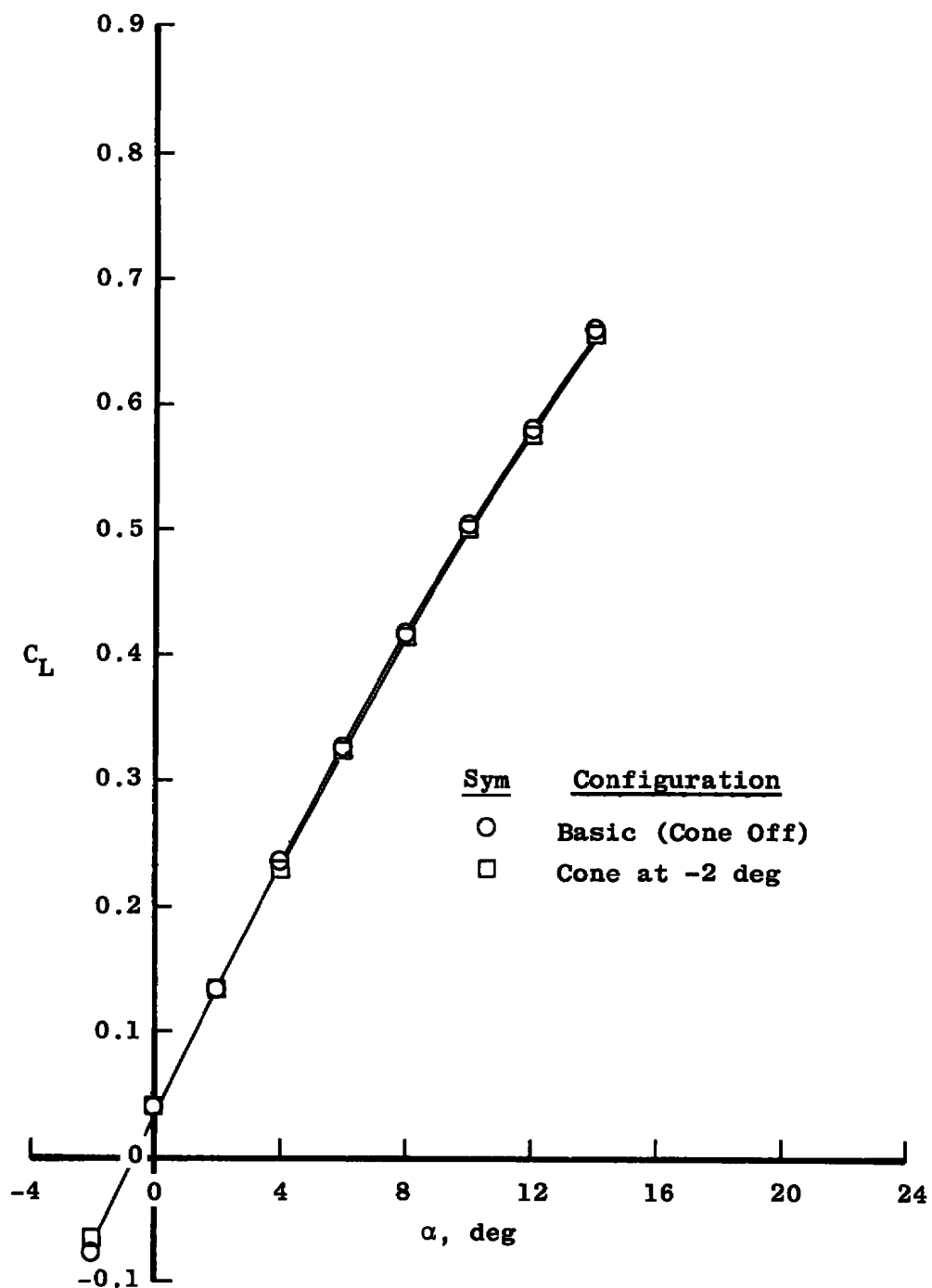
h. $M_\infty = 1.50$
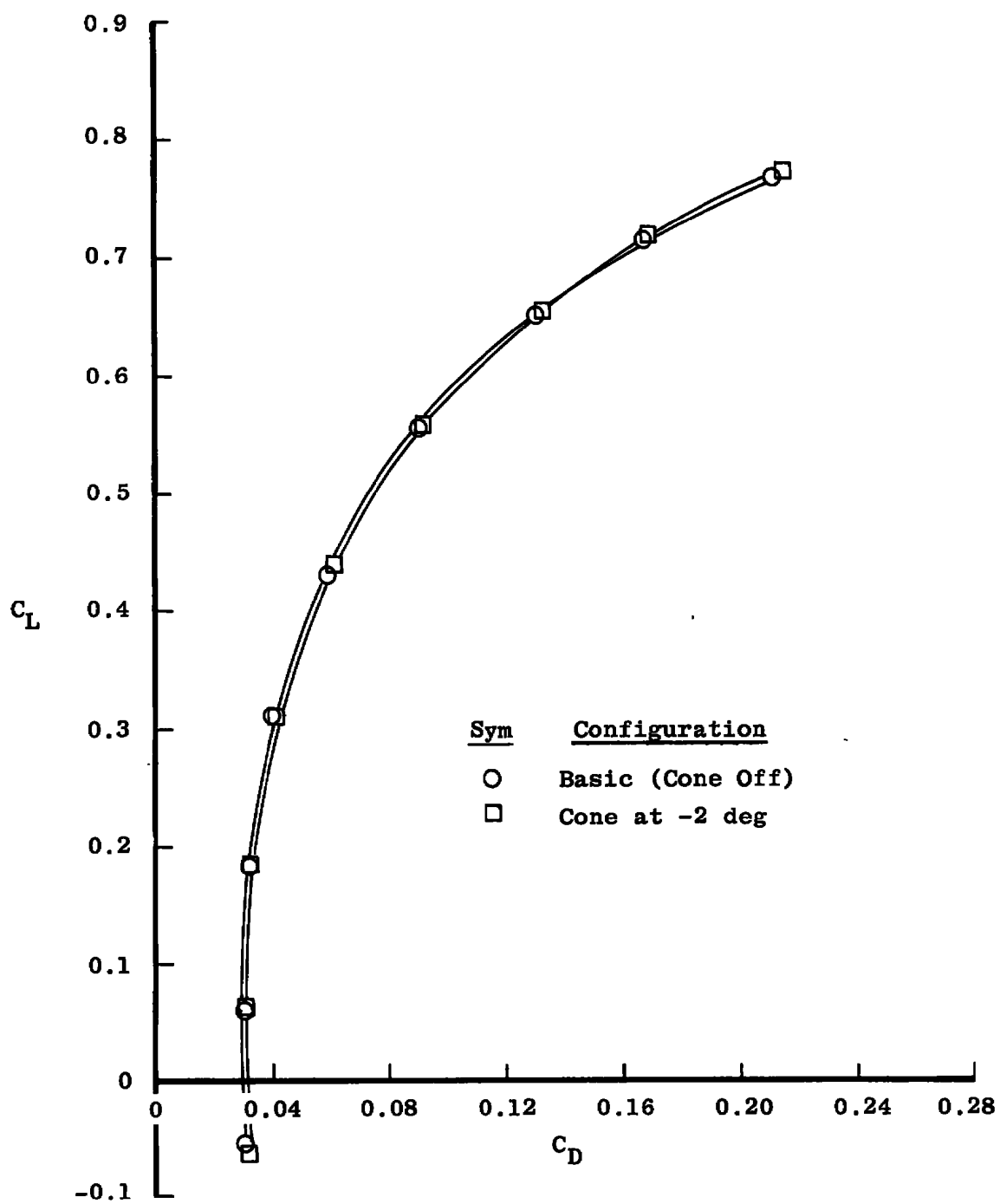Figure 6. Concluded.

a. $M_\infty = 0.20$

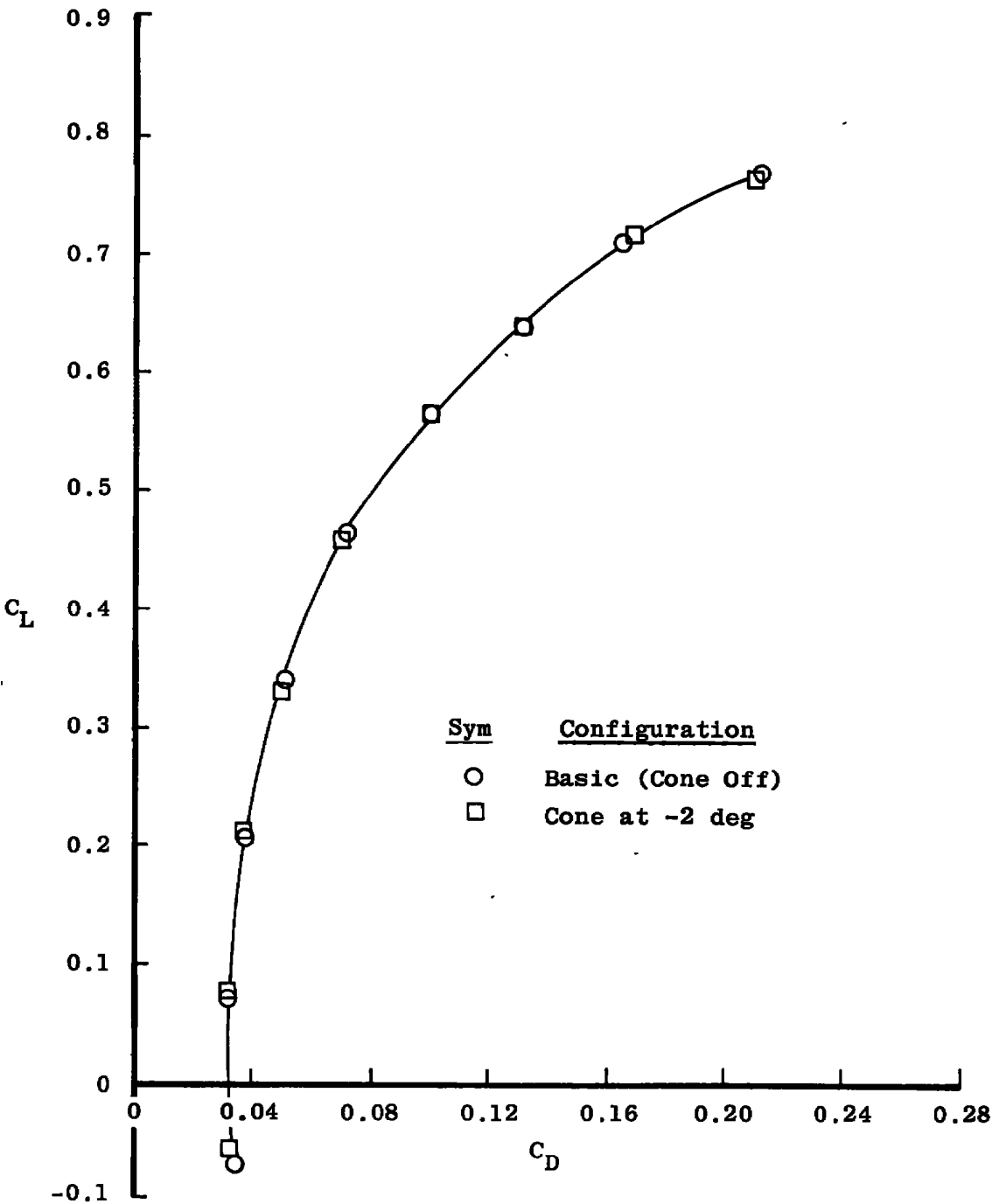Figure 7. Lift-drag curve at zero pitching moment.
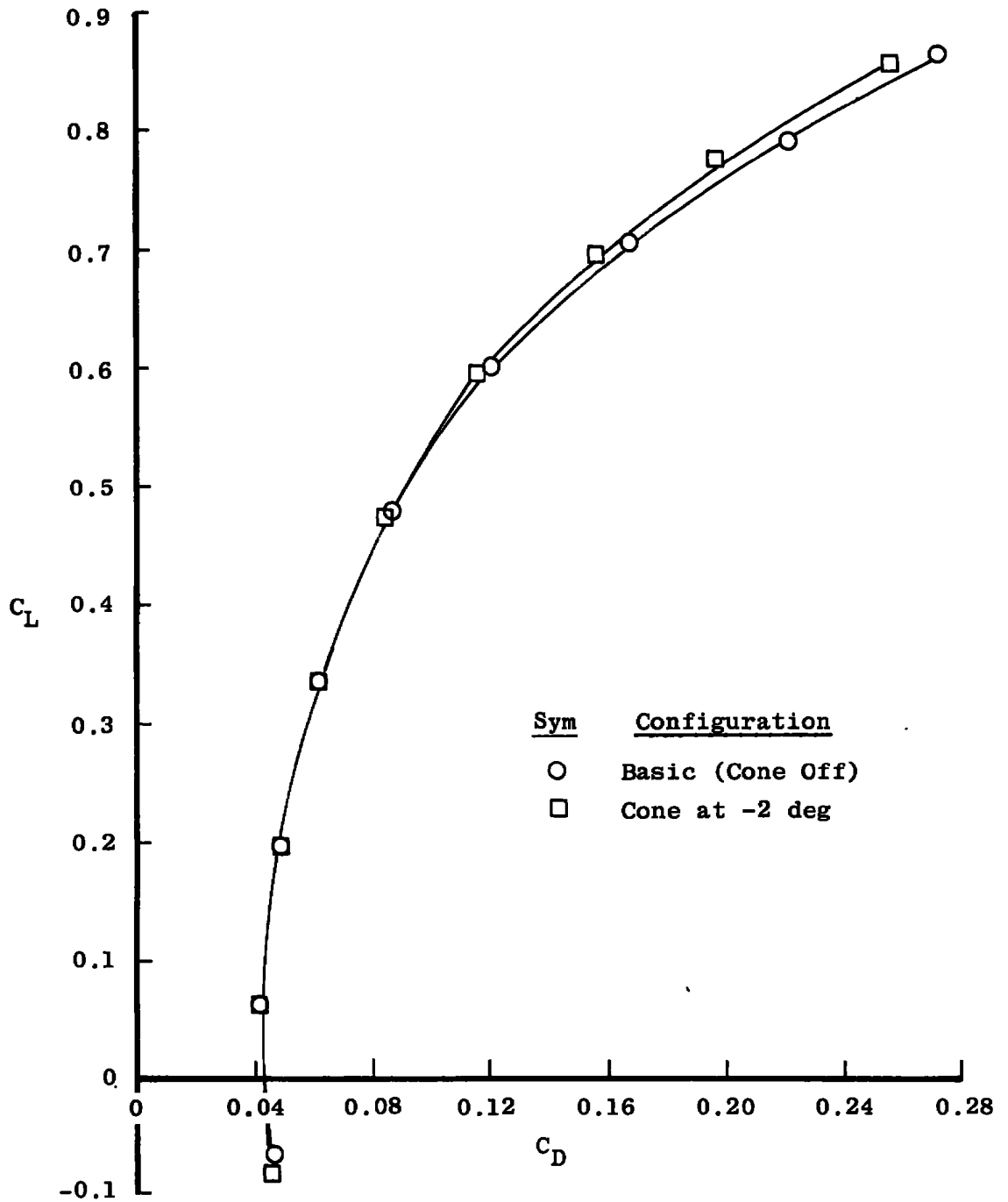
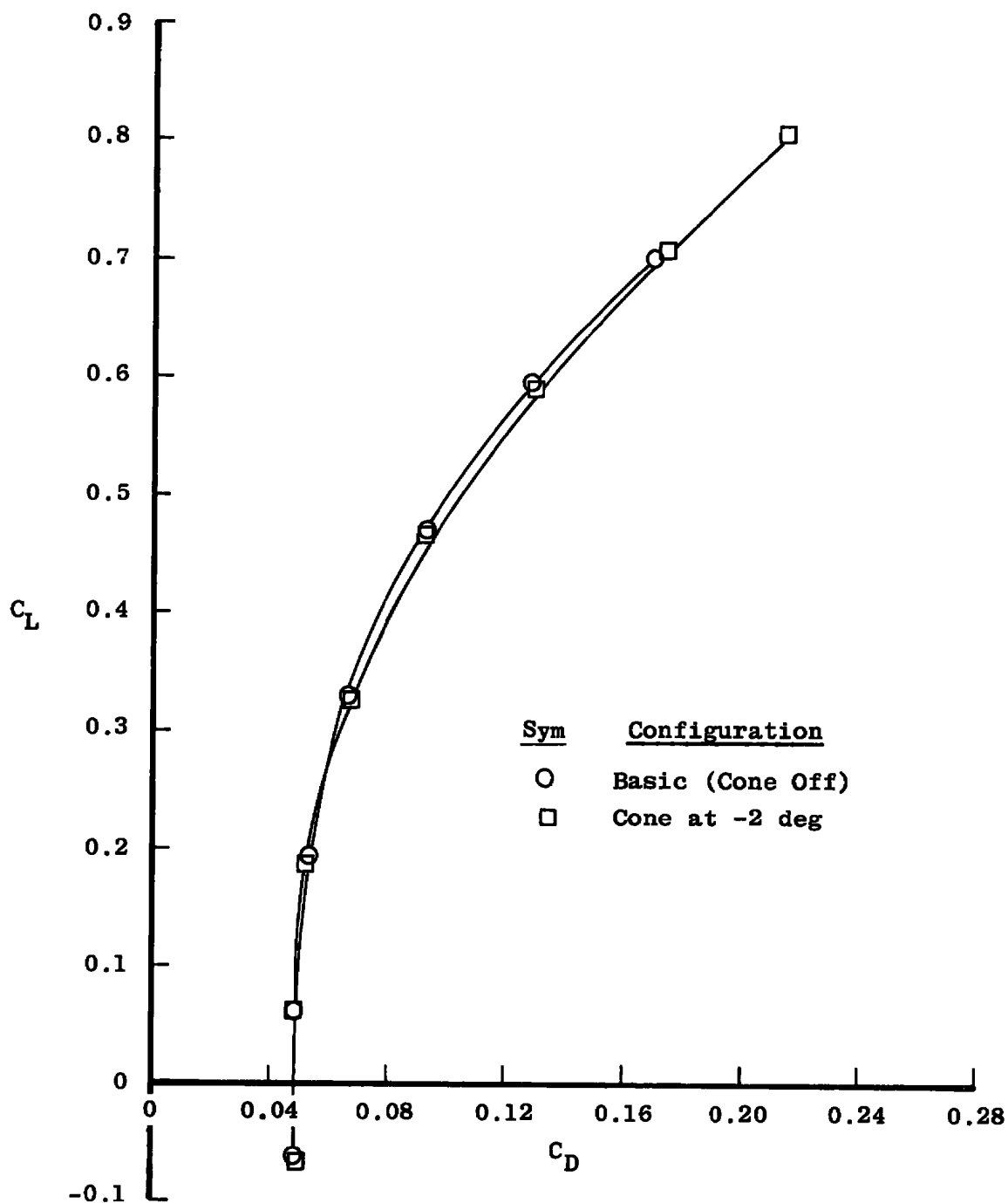b. $M_\infty = 0.60$
Figure 7. Continued.

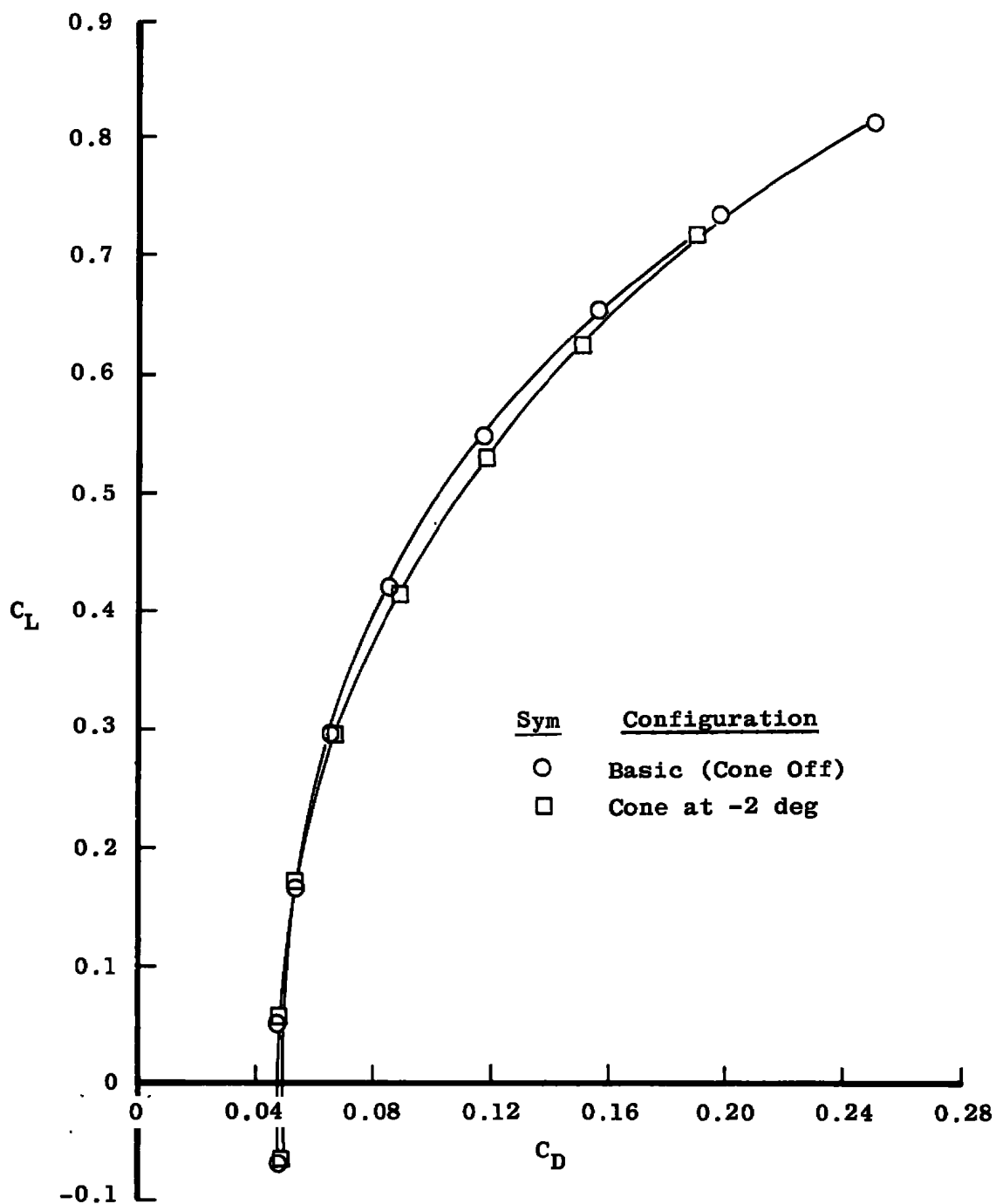c. $M_\infty = 0.80$
Figure 7. Continued.
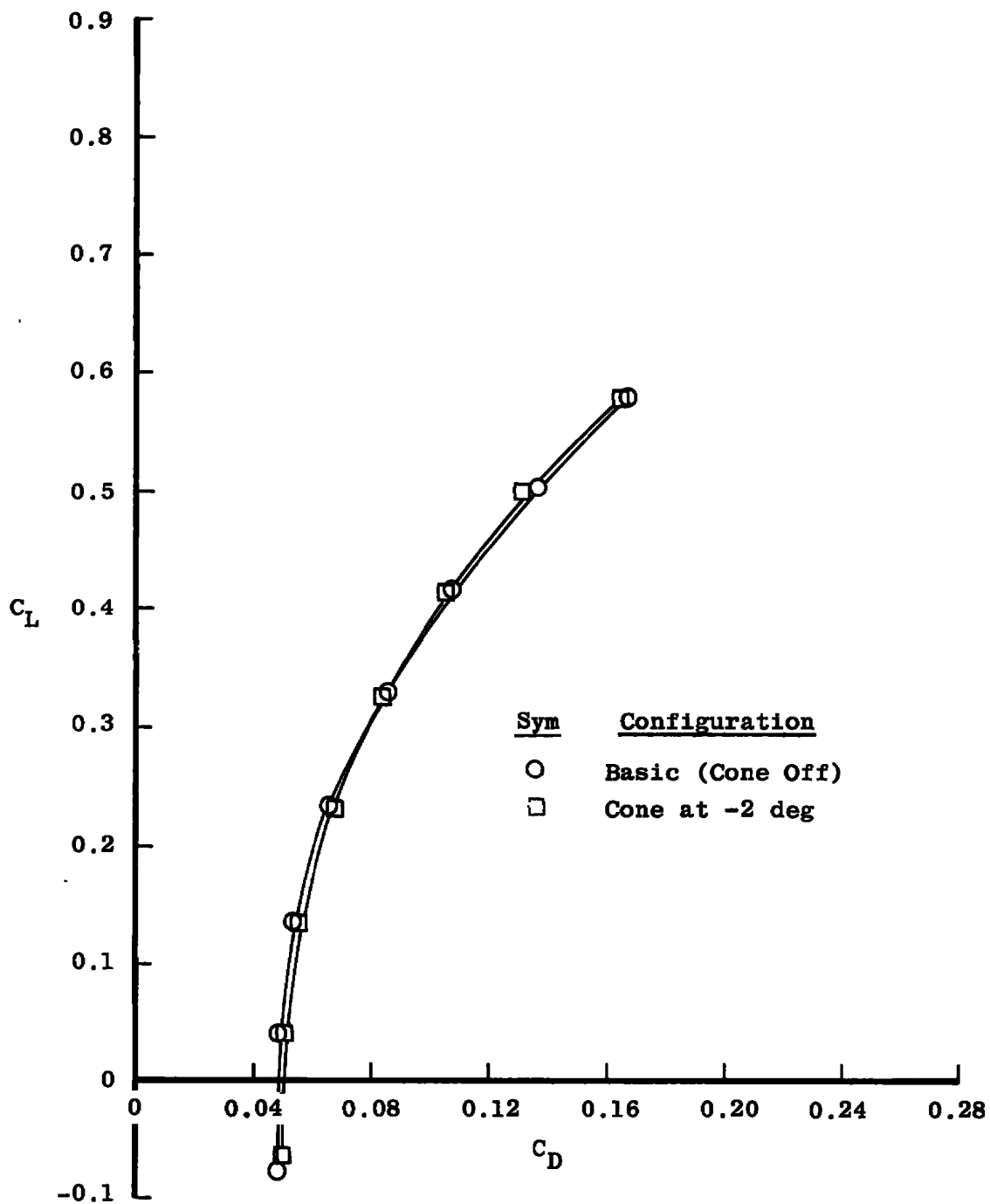
d. $M_\infty = 0.90$
Figure 7. Continued.

e. $M_\infty = 0.97$
Figure 7. Continued.

f. $M_\infty = 1.05$
Figure 7. Continued.

g. M_∞ = 1.20
Figure 7. Continued.

h. $M_\infty = 1.50$
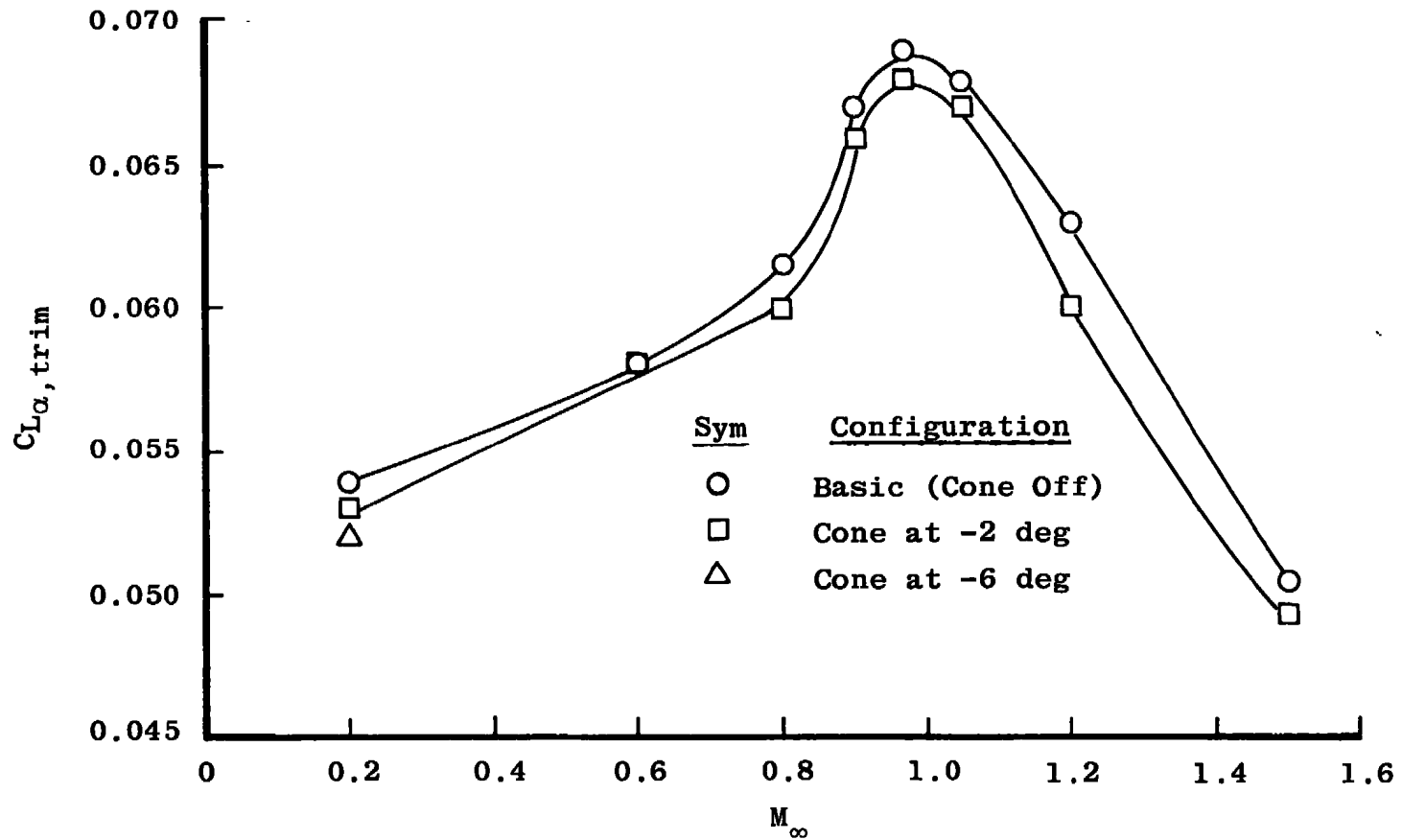Figure 7. Concluded.

Figure 8. Slope of the trim lift coefficient with angle of attack as a function of free-stream Mach number.

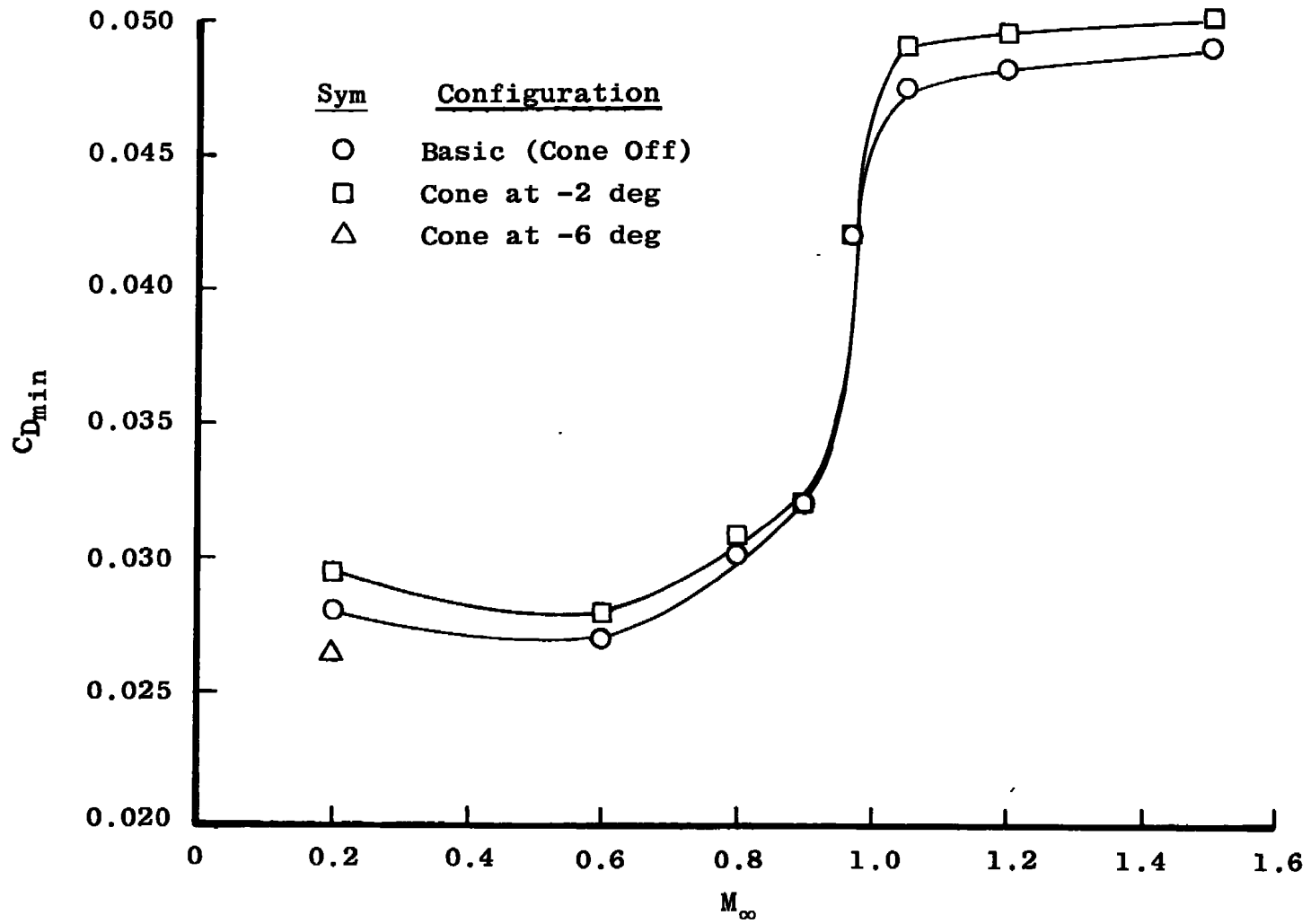Figure 9. Minimum drag coefficient as a function of free-stream Mach number.

Figure 10. Trim angle of attack as a function of free-stream Mach number.
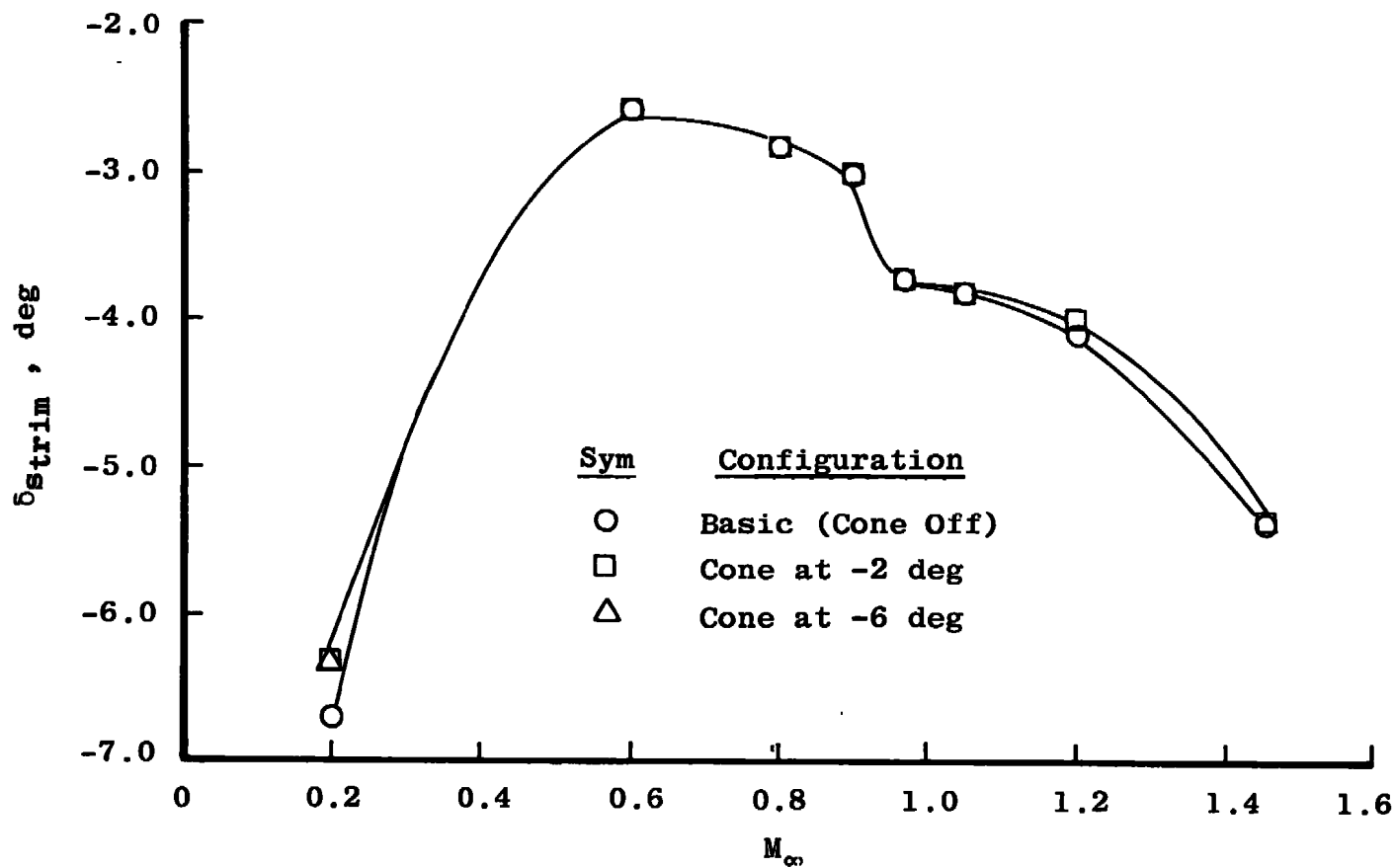
Figure 11. Stabilator trim angle as a function of free-stream Mach number.

Figure 12. Slope of pitching-moment coefficient versus angle of attack
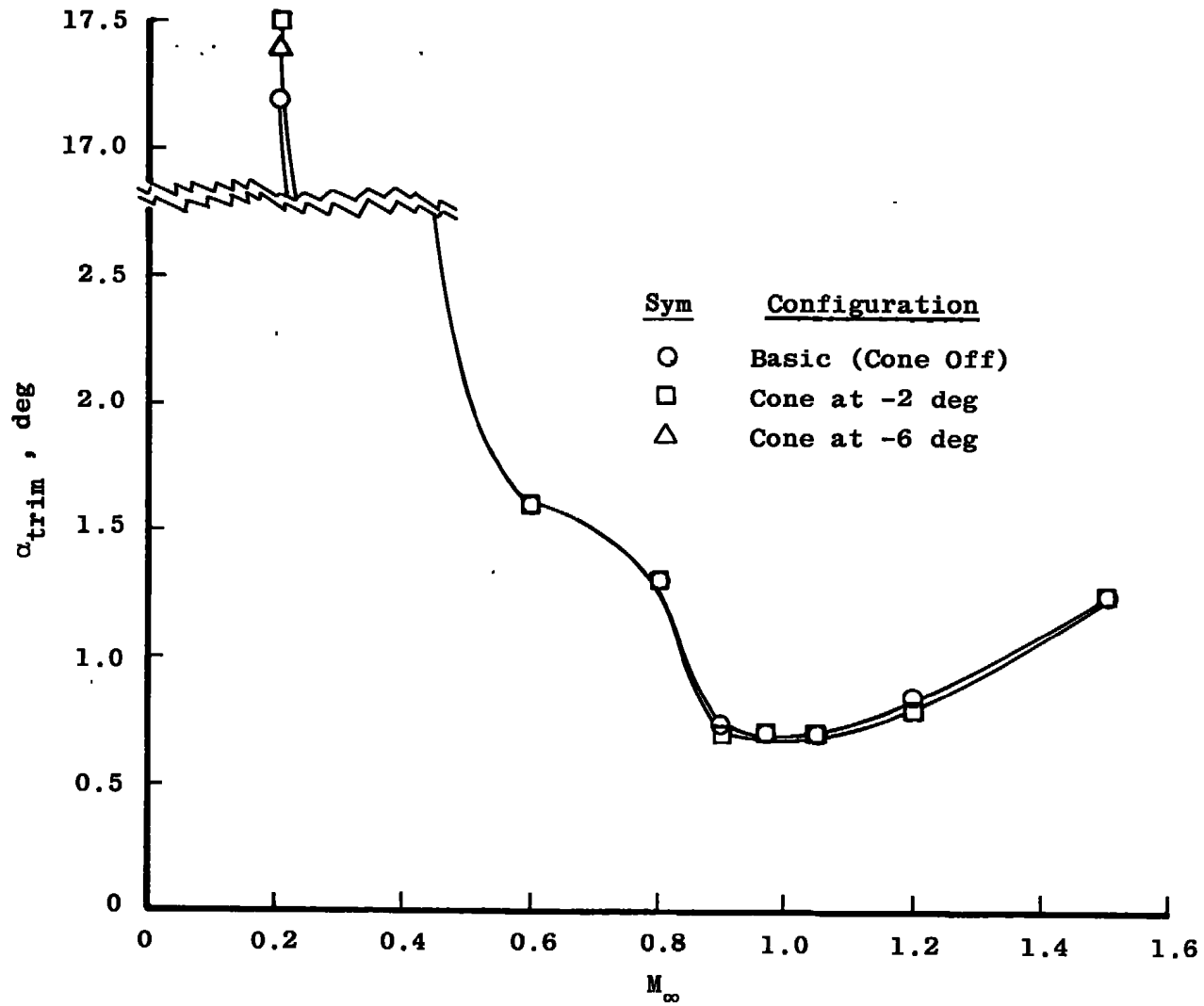as a function of free-stream Mach number.

Figure 13. Static margin as a function of free-stream Mach number.
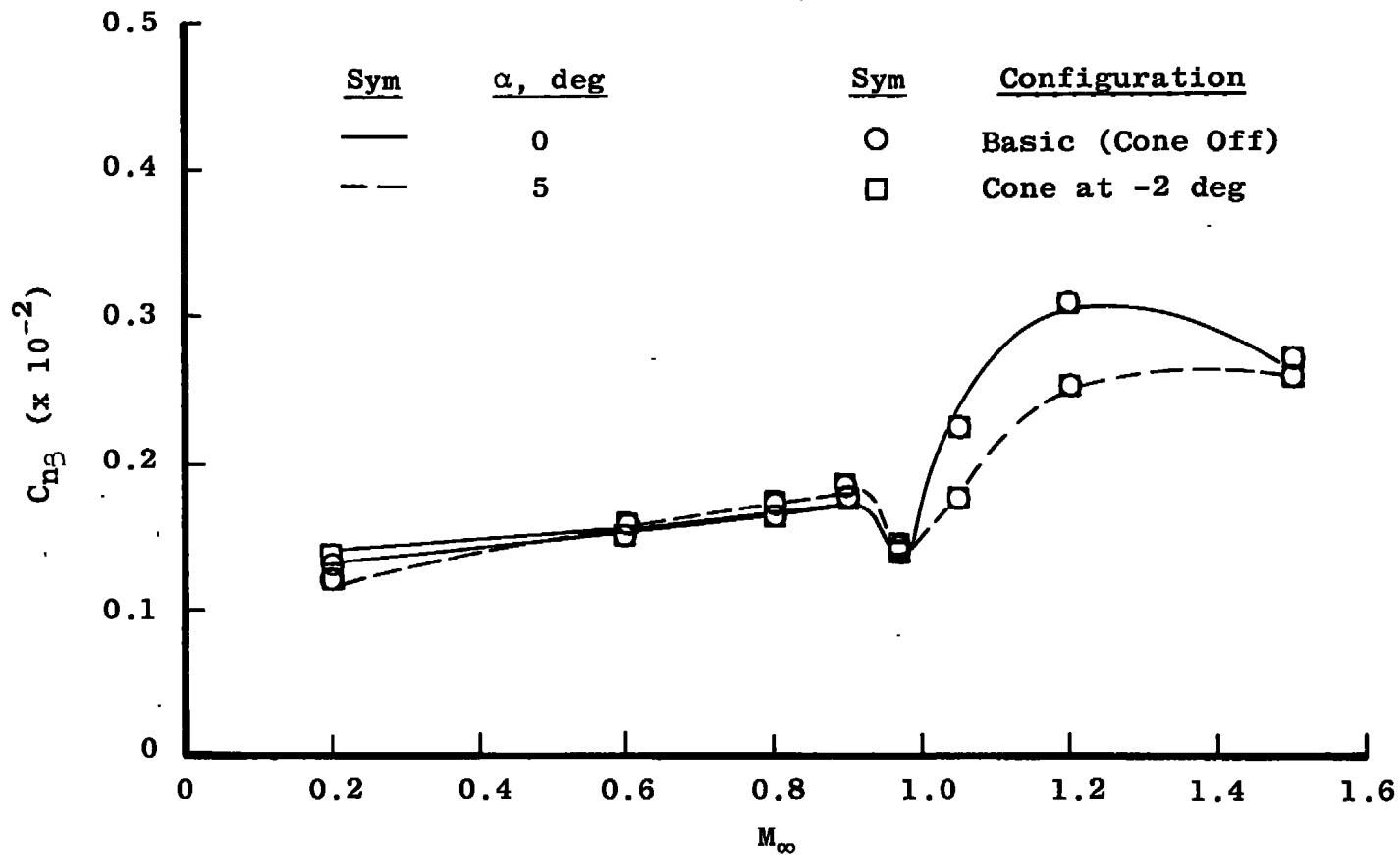
a. $|\beta| < 2$ deg

Figure 14. Slope of the yawing-moment coefficient versus sideslip angle
as a function of free-stream Mach number.
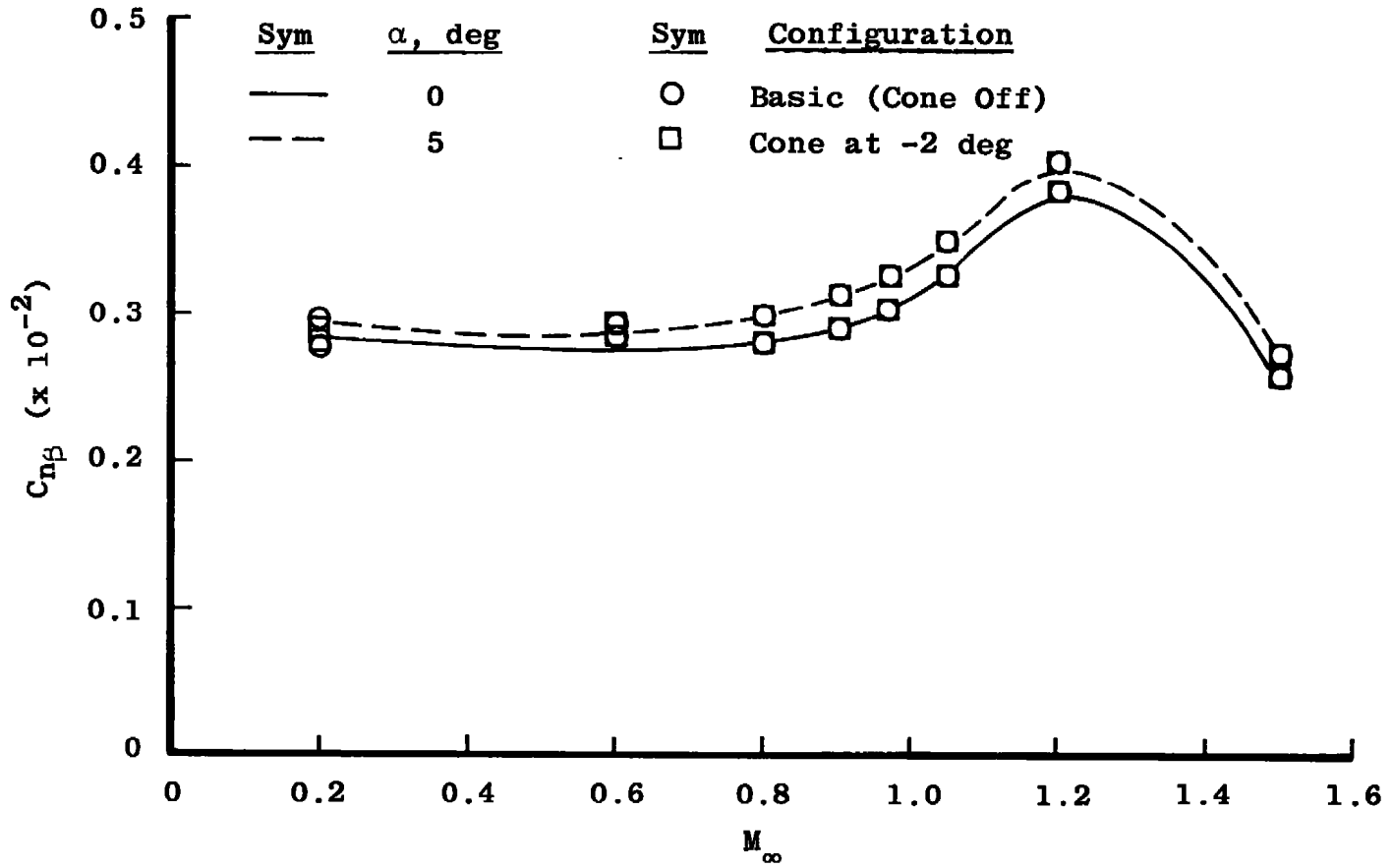
b. $|\beta| > 2$ deg
Figure 14. Concluded.
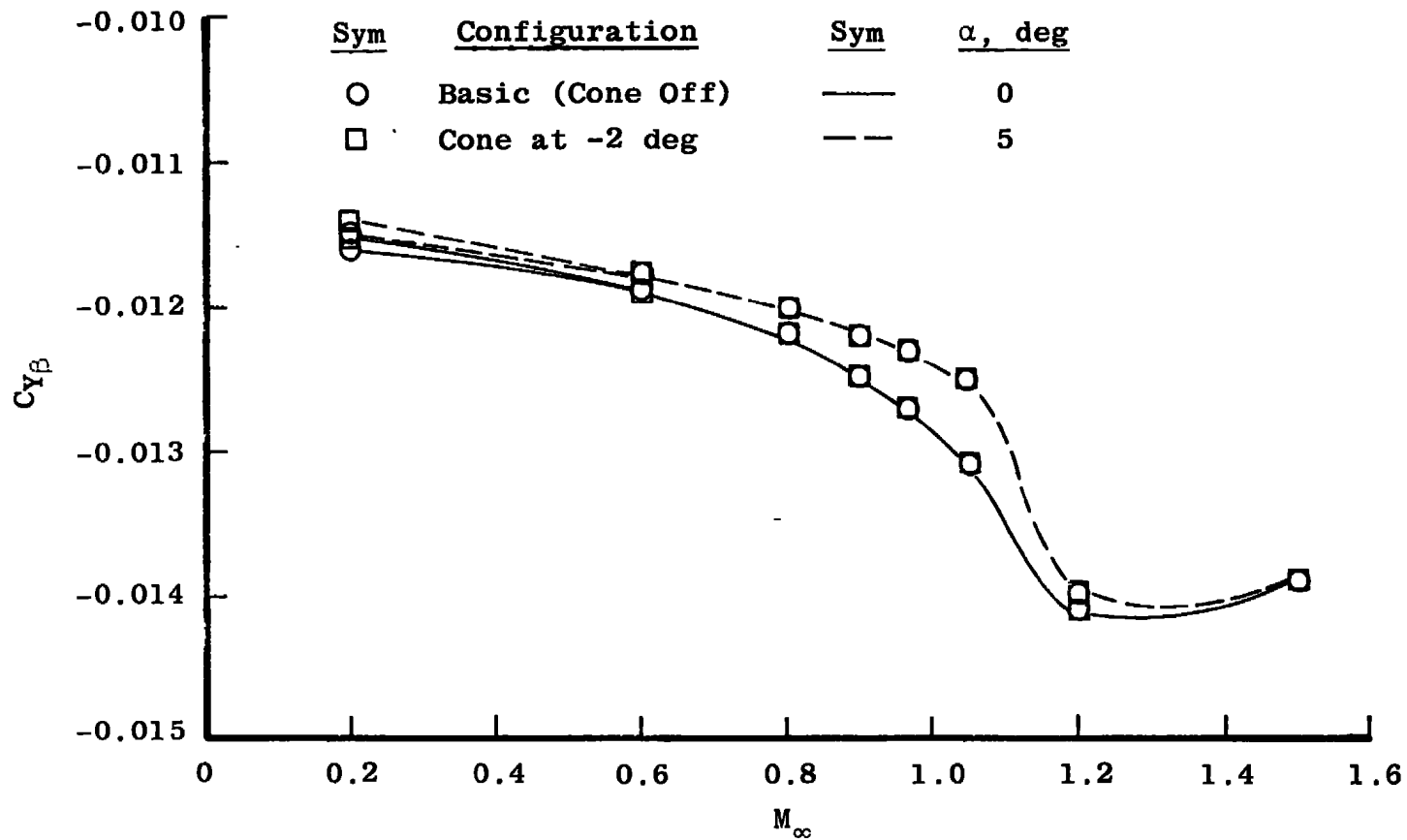
Figure 15. Slope of the side-force coefficient versus sideslip angle
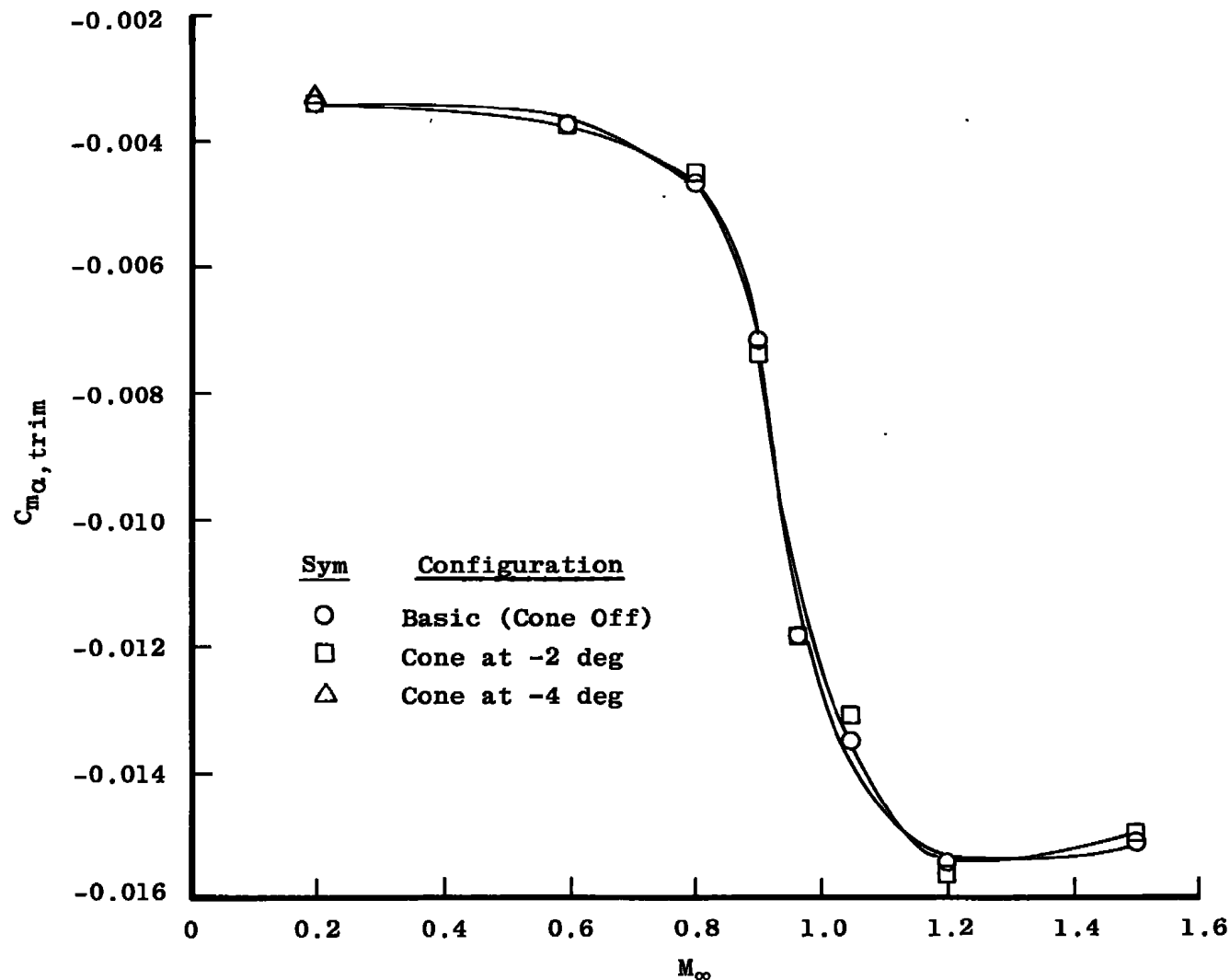as a function of free-stream Mach number.
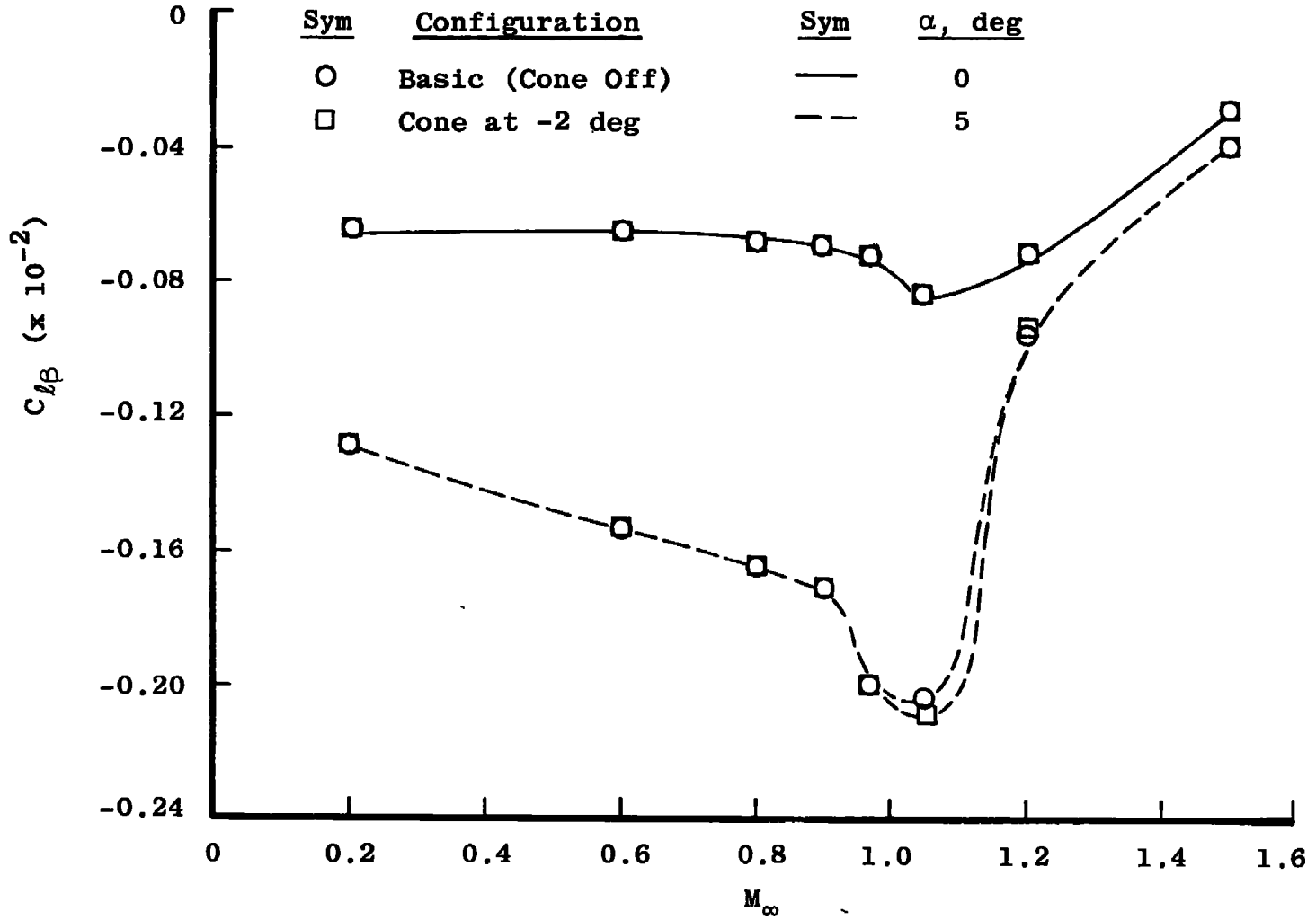
Figure 16. Slope of the rolling-moment coefficient versus angle of sideslip
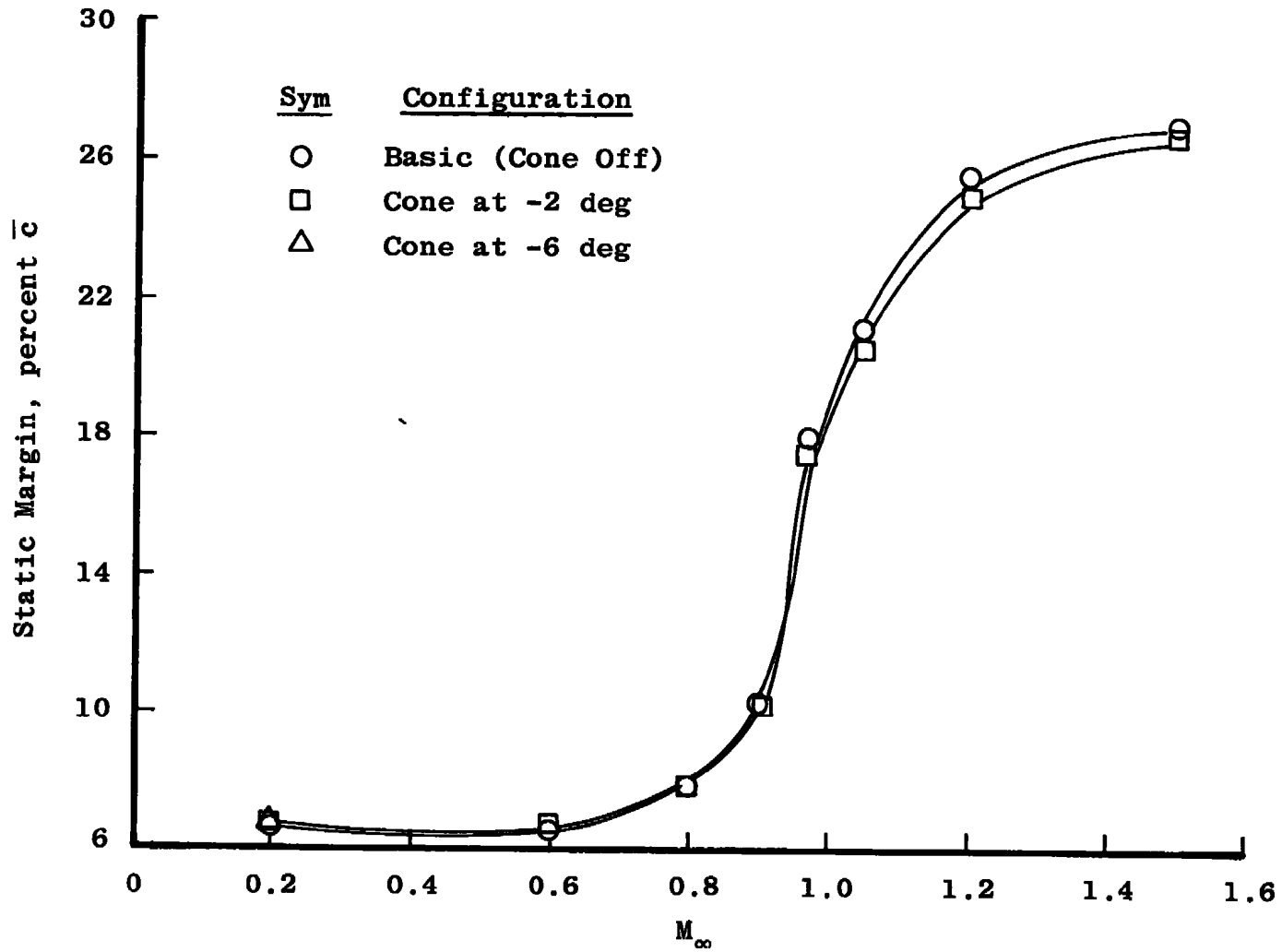as a function of free-stream Mach number.

Table 1. Free-Stream Parameter Uncertainties

M_∞	$\pm\Delta M_\infty$	$\pm\Delta p_t$, psfa	$\pm\Delta p_\infty$, psfa	$\pm\Delta q_\infty$, psf
0.20	0.0008	3.3	3.29	0.70
0.60	0.0023	2.2	3.60	2.68
0.80	0.0031	1.9	4.64	2.88
0.90	0.0042	1.8	4.92	2.98
0.97	0.0051	1.7	5.61	2.99
1.05	0.0140	1.7	14.32	6.50
1.20	0.0100	1.7	9.04	2.75
1.50	0.0105	1.6	6.80	1.12

Table 2. Balance Measurement Uncertainties

M_∞	α, deg	ΔC_L	ΔC_D	ΔC_m	ΔC_Y	ΔC_ℓ	ΔC_n
0.20	0	0.0505	0.0076	0.0233	0.0154	0.0049	0.0053
0.20	12	0.0499	0.0126	0.0233	0.0154	0.0049	0.0053
0.20	24	0.0474	0.0217	0.0234	0.0154	0.0049	0.0053
0.60	0	0.0100	0.0015	0.0046	0.0031	0.0010	0.0011
0.60	12	0.0104	0.0030	0.0046	0.0031	0.0010	0.0011
0.80	0	0.0088	0.0013	0.0037	0.0025	0.0008	0.0008
0.80	12	0.0080	0.0026	0.0037	0.0025	0.0008	0.0009
0.90	0	0.0082	0.0012	0.0034	0.0023	0.0007	0.0008
0.90	12	0.0074	0.0025	0.0034	0.0023	0.0007	0.0008
0.97	0	0.0082	0.0012	0.0034	0.0022	0.0007	0.0008
0.97	12	0.0072	0.0026	0.0033	0.0022	0.0007	0.0008
1.05	0	0.0079	0.0012	0.0033	0.0021	0.0007	0.0007
1.05	12	0.0068	0.0026	0.0032	0.0021	0.0007	0.0007
1.20	0	0.0067	0.0011	0.0029	0.0019	0.0006	0.0007
1.20	12	0.0062	0.0023	0.0028	0.0019	0.0006	0.0007
1.50	0	0.0062	0.0011	0.0029	0.0019	0.0006	0.0007
1.50	12	0.0062	0.0021	0.0029	0.0019	0.0006	0.0007

Table 3. Tunnel Conditions During Test

M_∞	p_t, psfa	T_t, $^\circ F$	q_∞, psf	Re/ft x 10^{-6}
0.20	2393	80	65.2	1.5
0.60	2236	100	441.8	3.5
0.80	1878	100	464.4	3.5
0.90	1782	100	597.3	3.5
0.97	1738	100	626.0	3.5
1.05	1703	100	654.3	3.5
1.20	1676	100	696.7	3.5
1.50	1636	100	701.8	3.3

NOMENCLATURE

A_b	Reference area of model base used in calculating forebody coefficients (0.07465 sq ft)
A_{cav}	Reference area of model cavity used in calculating forebody coefficients (0.0172 sq ft)
b	Reference width of model upon which aerodynamic coefficients are based (1.933 ft - model/38.666 ft - full scale)
C_D	Drag coefficient
$C_{D_{min}}$	Drag coefficient at its minimum value
C_L	Coefficient of lift
C_{L_α}	Change in lift coefficient with angle of attack
C_ℓ	Rolling-moment coefficient
C_{ℓ_β}	Change in rolling-moment coefficient with angle of sideslip
C_m	Pitching-moment coefficient
C_{m_α}	Change in pitching-moment coefficient with angle of attack
C_n	Yawing-moment coefficient
C_{n_β}	Change in yawing-moment coefficient with angle of sideslip
C_Y	Side-force coefficient
C_{Y_β}	Change in side-force coefficient with angle of sideslip
$\bar{c}$	Reference mean aerodynamic chord length of model upon which aerodynamic coefficients are based (0.802 ft - model/16.042 ft - full scale)
M_∞	Free-stream Mach number
p_t	Free-stream total pressure, psf

p_∞	Free-stream static pressure, psfa
q_∞	Free-stream dynamic pressure, psf
Re/ft	Unit Reynolds number
S	Reference area of model upon which aerodynamic coefficients are based (1.325 sq ft - model/530.00 sq ft - full scale)
SM	Static margin (percent chord)
T_t	Total temperature, °F
a	Angle of attack measured from model water reference line, deg
β	Model angle of sideslip, positive clockwise as viewed by the pilot, deg
δ_s	Horizontal stabilator deflection angle referenced to model water line, deg, positive when trailing edge is deflected downward